

## Benchmark Tests for Strong Ground Motion Simulations (Part 9: Theoretical Methods, Step 5 & 6)

MATSUMOTO, Toshiaki<sup>1\*</sup>, HISADA, Yoshiaki<sup>1</sup>, NAGANO, Masayuki<sup>2</sup>, NOZU, Atsushi<sup>3</sup>, ASANO, Kimiyuki<sup>4</sup>, MIYAKOSHI, Ken<sup>5</sup>

<sup>1</sup>Kogakuin University, <sup>2</sup>Tokyo University of Science, <sup>3</sup>The Port and Airport Research Institute, <sup>4</sup>Disaster Prevention Research Institute, <sup>5</sup>Geo-Research Institute

We have been conducting a series of benchmark tests of the strong motion simulation methods for three years since 2009. We chose the three most popular methods for this purpose: the theoretical methods (the wavenumber integration method, the discrete wavenumber method, and the thin-element method), the stochastic Green function method, and the numerical methods (the finite difference method and the finite element method). In this presentation (Part 9), we show the results of the theoretical methods for flat-layered structures in the step 5 and 6, and subsequent papers (Part 10) and (Part 11) show the results for numerical and empirical methods, respectively.

Show table 1, this table is list of Benchmark tests for the 2011 theoretical method (step 5 and 6). The step 5 and 6 use the Kanto sedimentary basin for the actual seismic sources (e.g., the 1990 West Kanagawa earthquake (M5.1) for step 5, and the 1923 Kanto earthquake (M7.9) for step 6). We selected 19 calculation points at the Kanto sedimentary basin from AIJ strong ground motion data sets, as shown figure 1. Structure models are flat-layered structures that extracted every 19 calculation points from 3D structure models.

All the results using various methods (the wavenumber integration method, the discrete wavenumber method, and the thin-layer method) generally show good agreements, as long as we use the same source and structure models. As compared with the observed records, those results generally simulate the body waves very well, but not the basin-induced surface waves.

Please check the following web site for more details.  
<http://kouzou.cc.kogakuin.ac.jp/benchmark/index.htm>

### Acknowledgements:

This project is in part supported by a research fund of Ministry of Education, Culture, Sports, Science and Technology of Japan (MEXT), and the Research Center of Urban Disaster Mitigation (UDM) of Kogakuin University. Toshiaki SATO, Nobuyuki YAMADA and Reiji KOBAYASHI, for providing us source model data.

**Keywords:** Strong Ground Motion Simulations, Benchmark Test, Theoretical Methods, Wavenumber Integration Method, Discrete Wavenumber Method, Thin Layer Method

Table 1 Benchmark tests for the 2011 theoretical method (step 5 and 6)

名称	1990年西武池袋線西武池袋駅付近の地震 (M5.1)	1990年伊豆大島近海の地震 (M6.6)	1923年関東大震災 (M7.9)
震源	136.0°E, 35.8°N	139.2°E, 34.9°N	139.7°E, 35.8°N
震源深さ	10km	10km	10km
震害	関東平野の北東部関東平野の北東部	関東平野の北東部	関東平野の北東部
震害記録	0~0.33 Hz (0.5秒以上)	0~0.33 Hz (0.5秒以上)	0~0.33 Hz (0.5秒以上)
出力点	19地点 (AIJデータベースから19地点を本報告書に)	19地点 (AIJデータベースから19地点を本報告書に)	19地点 (AIJデータベースから19地点を本報告書に)

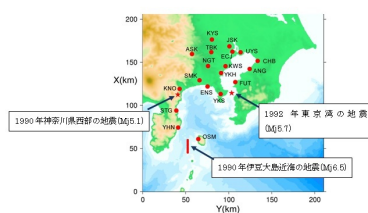


Figure 1 Location of Hypocenter and calculation points (step 5)

## Benchmark Tests for Strong Ground Motion Simulations (Part 10: Numerical Methods, Step 5 & 6)

YOSHIMURA, Chiaki<sup>1\*</sup>, NAGANO Masayuki<sup>2</sup>, HISADA Yoshiaki<sup>3</sup>, AOI Shin<sup>4</sup>, IWAKI Asako<sup>4</sup>, KAWABE Hidenori<sup>5</sup>, HAYAKAWA Takashi<sup>6</sup>, Seckin Ozgur CITAK<sup>7</sup>

<sup>1</sup>Taisei Corporation, <sup>2</sup>Tokyo University of Science, <sup>3</sup>Kogakuin University, <sup>4</sup>NIED, <sup>5</sup>Kyoto University, <sup>6</sup>Shimizu Corporation, <sup>7</sup>JAMSTEC

### 1. Introduction

We have been conducting a benchmark test for strong motion simulation methods with numerical methods (finite difference method and finite element method). During 3 years of the research period, we studied 14 problems categorized in 6 steps with various degree of complexity from a simple homogeneous model to a realistic Kanto basin model.

In step 1, we studied a homogeneous model and a two-layer model with a point source. In step 2, we studied the two-layer model with extended source models: a lateral fault and a reverse fault. (Yoshimura et al., 2011). In step 3 and 4, we considered a four-layer model, a symmetric trapezoidal basin model and an asymmetric slant-basement basin model (Yoshimura et al., 2012). In this report, we present the results of step 5 and 6 in which we considered a realistic Kanto basin model where Tokyo metropolitan area is located.

### 2. Problems for step 5 and 6

We considered a 3-dimensional Kanto basin model and the source models of 4 observed earthquakes. Six teams participated in this year. Table 1 shows the calculation conditions. Figure 1 shows the calculation domain (210km x 270km) with source model (stars or circles) and calculation sites (squares).

In step 5, we targeted 3 small or middle earthquakes: 1990 Western Kanagawa Prefecture earthquake (Mj 5.1), 1990 Near Izu-Oshima earthquake (Mj6.5) and 1992 Tokyo bay earthquake (Mj 5.7). We constructed the source models based on Sato T. et al. (1998) and Yamada and Yamanaka (2003).

We constructed the 3-dimensional Kanto Basin model based on the model proposed by The Headquarter for Earthquakes Research Promotion (2009). The grid size or element size were set so that the calculation results are effective at the frequency domain from 0 to 0.33 Hz. Participants turned in calculated velocity time history data for 19 sites.

In step 6, we targeted 1923 Kanto earthquake (Mj 7.9). The source model was constructed based on the inverted source model proposed by Sato H. et al. (2005).

### 3. An example of calculated results

Figure 2 shows the calculated Y (EW) component of velocity waves at ASK. Yoshimura calculated with FEM. Nagano, Hayakawa, Citak et al., Iwaki et al. and Kawabe calculated with FDM. In addition, Fig.2 shows Hisada's result calculated with a wave number integration method considering a flat layered model. Because ASK is a rock site, the waveform is simple. The results by FEM and FDM agree with each other. Hisada's result is similar to those results because the seismic wave mainly consists of body wave and the flat layer approximation is effective. On the other hand, at the sites on the thick sedimentary basin, the later phases induced by basin structure become dominant. Our results on sedimentary sites show generally good agreement but are not as perfect as ASK at the present moment. We are now checking reasons such as the difference of modeling of surface thin layer and are planning to revise the results.

For more details, please check <http://kouzou.cc.kogakuin.ac.jp/benchmark/index.htm>

### Acknowledgement

This project is partly supported by a research fund of Ministry of Education, Culture, Sports, Science and Technology of Japan (MEXT), and the Research Center of Urban Disaster Mitigation (UDM) of Kogakuin University. We would like to thank Dr. Toshiaki SATO, Dr. Nobuyuki YAMADA and Dr. Reiji KOBAYASHI for providing us source model data. We would like to thank Dr. Shinichi MATSUSHIMA and Dr. Robert W. GRAVES for participating in Citak's team.

### References

- 1) Yoshimura et al., AIJ J. Technol. Des. Vol.17, Mo.35, 67-72, Feb.,2011. (in Japanese)
- 2) Yoshimura et al., AIJ J. Technol. Des. Vol.18, Mo.38, 95-100, Feb.,2011. (in Japanese)
- 3) Sato T. et al., Bull. Seism. Soc. Am., Vol. 88, No1, pp.183-205, Feb., 1998.

SSS26-02

Room:304

Time:May 20 09:15-09:30

- 4) Yamada and Yamanaka, Zisin 2, Vol. 56, 111-123, 2003. (in Japanese)
- 5) The Headquarter for Earthquakes Research Promotion, 2009. [http://www.jishin.go.jp/main/chousa/09\\_choshuki/](http://www.jishin.go.jp/main/chousa/09_choshuki/)
- 6) Sato H. et al., Science, 309, 462-464, 2005.

Keywords: Fault model, Finite element method, Finite difference method, Kanto plain, Kanto earthquake, Western Kanagawa Prefecture earthquake

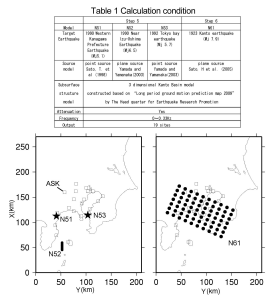


Fig.1 Calculation domain, seismic sources and output sites

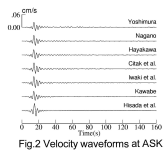


Fig.2 Velocity waveforms at ASK

## Benchmark Tests for Strong Ground Motion Simulations (Part 11:Stochastic Green's Function Method, Step 5 & 6)

KATO, Kenichi<sup>1\*</sup>, HISADA Yoshiaki<sup>2</sup>, OHNO Susumu<sup>3</sup>, NOBATA Arihide<sup>4</sup>, MORIKAWA Atsushi<sup>1</sup>, YAMAMOTO Yu<sup>5</sup>

<sup>1</sup>Kobori Research Complex Inc., <sup>2</sup>Kogakuin Univ., <sup>3</sup>Tohoku Univ., <sup>4</sup>Obayashi Co., <sup>5</sup>Taisei Co.

Benchmark tests for the strong motion simulation methods have been performed as three years project since 2009. This paper focuses on the results using stochastic Green's function method.

We have carried out simple benchmark tests in 2009; one is a point source (step 1) and the other is extended sources (step 2) in homogeneous and two-layered subsurface structures. Radiation coefficient of the source is assumed to be frequency independent, and only SH wave is considered. Site amplification is calculated assuming normal incidence of SH wave. Six groups of researchers/engineers were participated in by using their own methods/codes. Since the simple model is used in the steps 1 and 2, all the results calculated by six teams generally show good agreements to each other (Kato et al., 2011). In steps 3 (point source) and 4 (extended source), more complicated analytical conditions are considered. For example, frequency dependent radiation coefficient of the source is applied. Since oblique incidences of both SH and SV waves are considered, vertical component is also generated in addition with horizontal components. All the results of the point sources and the extended sources from five participants generally show good agreements to each other in spite of complicated analytical conditions. Synthesized amplitude shows variation in particular frequencies, because random numbers are used in generating time histories. When applying the stochastic Green's function method, this variation should be in mind (Kato et al., 2012).

In the steps 5 and 6, the Kanto sedimentary basin for the 1923 Kanto earthquake (M7.9) is considered as an actual source and structure model. Variable slip model by Sato et al. (2005) is characterized to two asperities and background regions as shown in Fig.1. Table 1 shows analytical condition. The model S51 in Table 1 assumes the point source located within the asperity 1. Since random numbers used in generating time histories are given in advance, synthesized strong ground motions at ASK and ECJ from all four participants coincide with each other. This agreement indicates that the frequency dependent radiation coefficient of the source is properly applied and site response by oblique incidences of both SH and SV is accurately calculated. The model S61 in Table 1 assumes extended source and strong ground motions are synthesized at 4 sites. The response spectra from four participants show good agreement to each other. The response spectra are also compared with those from empirical attenuation model. Although the response spectra shorter than 0.2 sec correspond with each other, the spectra longer than 0.2 sec from stochastic Green's function method show systematically smaller amplitude than that from empirical attenuation model. By comparing the synthesized strong motions from theoretical method such as the wavenumber integration method and thin layer method under the same subsurface structure, the applicability of hybrid approach will be discussed. Please check the following web site for more details.

<http://kouzou.cc.kogakuin.ac.jp/test/home.htm>

### Acknowledgments:

This project is in part supported by a research fund of Ministry of Education, Culture, Sports, Science and Technology of Japan (MIEXT), the Research Subcommittees on the Earthquake Ground Motion of the Architectural Institute of Japan, and the Research Center of Urban Disaster Mitigation (UDM) of Kogakuin University.

### References:

Kato et al., Benchmark tests for strong ground motion prediction methods: Case for stochastic green's function method (Part 1), AIJ J. Technol. Des. Vol. 17, No.35, 49-54, 2011.

Kato et al., Benchmark tests for strong ground motion prediction methods: Case for stochastic green's function method (Part 2), AIJ J. Technol. Des. Vol. 18, No.38, 67-72, 2012.

Sato et al., Earthquake source fault beneath Tokyo, Science, 309, 462-464, 2005.

**Keywords:** Strong motion prediction methods, Benchmark tests, Stochastic Green's function method, Random numbers, Point source, Fault model

SSS26-03

Room:304

Time:May 20 09:30-09:45

Table 1 Benchmark tests for stochastic green's function method

モデル名	ステップ5 (点震源)		ステップ6 (面震源)	
	S51 (必須)	S52 (必須)	S61 (必須)	S62 (任意)
対象地震	1923年関東地震(Mj7.9)のアスぺリティ		1923年関東地震(Mj7.9)	
震源のモデル化	アスぺリティ内の1要素を点震源として用いる		Sato <i>et al.</i> (2005)のすべり分布の特性化モデル	Sato <i>et al.</i> (2005)のすべり分布を使用した不均質モデル
地盤	関東平野の3次元深部地盤モデル(長周期地震動予測モデル、2009試作版)を用い、観測点直下の平行成層地盤を使用			
減衰	あり			
乱数位相	指定	各自の乱数位相3パターン		
有効振動数	0~20Hz			
出力点	4地点(岩盤サイト:浅川、堆積層サイト:清瀬、越中島、本郷)			

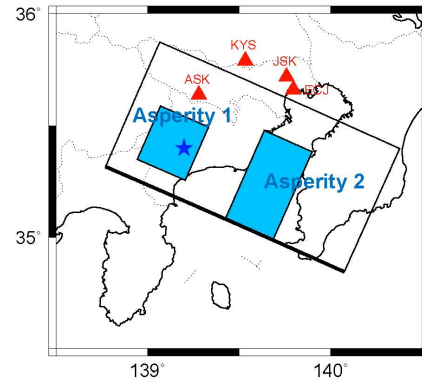


Fig. 1 Characterized fault model and stations for calculation

## Correction for slip function and its implications

MASUDA, Tetsu<sup>1\*</sup>

<sup>1</sup>ERI

Green's function method is useful for simulating strong ground motion. It is necessary to correct for the amplitude and dominant period difference between the bigger target earthquake and the small earthquake as the Green's function. Correction is based on the scaling relations that the slip rise time, as well as slip amount, is scaled by the source dimension. Correction functions of particular type have been proposed. Boxcar type function (Irikura, 1983), exponential time function (Onishi and Horike 2004) for slip velocity time function, or two-order rational function for radiated wave spectrum (Dan and Sato, 1998) is assumed to derive correction function, while Irikura (1986), Irikura et al.(1997), and Nozu (2002) directly specified the correction functions. The correction function spectrum takes a constant value  $N$ , which is the ratio of source dimension, in lower frequencies than a corner frequency  $f_t$  relating to the target rise time  $T$ , and it is unity in higher frequencies than another corner frequency  $f_g$  relating to the small earthquake rise time, and it falls off with increasing frequency between the two corners.

Seismic wave is evaluated by integrating slip velocity over the fault surface. Assuming the slip velocity is uniform over the rectangular fault and rupture propagates constantly, surface integral of slip velocity over a finite fault results in a product of two Sinc functions, one with argument of  $2\pi f T_x$ , and another with argument of  $2\pi f T_y$ , where  $T_x = (X/c - 1/V_x) \cdot L/2$ ,  $T_y = (Y/c - 1/V_y) \cdot W/2$ ,  $f$  is frequency,  $L$  and  $W$  the source dimension,  $X$  and  $Y$  the direction cosine,  $R$  the distance,  $c$  the phase velocity,  $V_x$  and  $V_y$  the rupture velocity. The spectrum is flat in lower frequencies than  $f_c$ , relating to square root of  $T_x \cdot T_y$ , and it falls off from the corner proportionally to the squared frequency.

In Green's function method, instead of integrating slip velocity, waves of small earthquakes located at discrete points are summed up. The spectrum of summation is also flat in lower frequencies than the corner  $f_c$ , and falls off similarly from  $f_c$ , however in this case, it increases from a frequency  $f_e = f_c/N$  and keeps a constant level in higher frequencies.

The corner frequency  $f_c$  is due to fault finiteness, and the spectrum decays from  $f_c$ . If the corner  $f_t$  is close to  $f_c$ , the spectrum of synthesized wave by means of Green's function method falls off between these two corners steeper than the omega-squared model because both of the correction function and summation over the fault. The rise time is in many cases set to  $W/2V_r$  referring to numerical simulations by Day (1982). In this case, the corner frequency  $f_t$  is close to  $f_c$ , and consequently underestimation of spectrum contents is resulted between these two corners. Kataoka et al.(2003) pointed out that the shorter rise time is consistent with the observations.

The rise time  $W/2V_r$  is an approximation of total duration of slip near the center of fault. The slip velocity steeply increases after rupture arrives and decrease in a short time after it reaches the peak, and the peak decreases to zero at fault edge. Many studies of source process indicate that the rise time is as short as one tenth of total duration of rupture  $L/V_r$ .

Uniform slip velocity over an asperity area is usually assumed in a characteristic source model. The rise time  $W/2V_r$  is too long if applied all over asperity area, and shorter rise time is appropriate for the proposed correction functions. The correction function by Onishi and Horike or Nozu is consistent with the impulsive feature of slip velocity. A large value of exponent coefficient is preferable since it approximates the numerical results. In order to properly estimate seismic wave spectrum independent of the size of the Green's function, it is necessary to set a shorter rise time or to take a large value of exponent coefficient.

Keywords: Green' function method, slip time function, correction function, rise time

## Quick estimation of moment magnitude based on real-time displacement waveform

HIRAI, Takashi<sup>1\*</sup>, FUKUWA, Nobuo<sup>1</sup>

<sup>1</sup>Environmental Studies, Nagoya University

### 1. Introduction

The 2011 off the Pacific coast of Tohoku Earthquake was the greatest earthquake in Japan as the magnitude of 9.0. But the first report of JMA (Japan Meteorological Agency) magnitude estimated at 3 minutes after initiation was 7.9. Furthermore, the moment magnitude which should be calculated at 15 minutes after initiation was not calculated due to the saturation of broad-band seismometers. As a result, the tsunami height was underestimated causing loss of many lives unfortunately. Now southwestern Japan faces a great earthquake of Nankai trough, so it is extremely important to construct the quick estimation system of unsaturated magnitude. Previously we developed a method to estimate the permanent displacement accurately based on an acceleration record<sup>1)</sup>. Applying the method, we propose a scheme to estimate moment magnitude quickly using the relation between the displacement and hypocenter distance.

### 2. Method

Relation between the permanent displacement  $u$  due to the earthquake and the hypocenter distance  $r$  is expressed as

$$u = M_0 A / Gr^2, \dots (1)$$

where  $M_0$  is the seismic moment,  $A$  is a coefficient to consider the direction effect,  $G$  is the rigidity. Taking the logarithm of eq. (1), we obtain

$$\log u = -2 \log r + \log ( M_0 A / G ) \dots (2)$$

Namely, plotting displacements versus hypocenter distances in double logarithmic chart, the seismic moment  $M_0$  can be calculated from the intercept of line of slope -2.

In this study, based on the acceleration waveform recorded by the strong ground motion observation network KiK-net, we obtained the displacement waveform and permanent displacement according to Hirai and Fukuwa (2012)<sup>1)</sup>. Applying this procedure to many observation point, the seismic moment and moment magnitude were calculated.

### 3. Result and discussion

The result for the 2011 off the Pacific coast of Tohoku Earthquake is shown in the Figure. Figure (a) shows the permanent displacement distribution, (b)-(g) show estimated values of the magnitude at each time, respectively. According to the Figure, it is found that the estimated value of the magnitude grows increasingly and that the earthquake can be obtained as  $M_w \sim 9$  class great at 4 minutes after the initiation. This value is consistent with that from the inversion of co-seismic crustal deformation observed by GPS network<sup>2)</sup>. Therefore, the availability of this method was suggested.

### References

- 1) T. Hirai and N. Fukuwa, Estimation of crustal deformation distribution due to the 2011 off the Pacific coast of Tohoku Earthquake based on strong motion records, *J. Struct. Constr. Eng., AIJ*, **77**, 341-350 (2012).
- 2) T. Ito, K. Ozawa, T. Watanabe, T. Sagiya, Slip distribution of the 2011 off the Pacific coast of Tohoku Earthquake inferred from geodetic data, *Earth Planets Space*, **63**, 627-630 (2011).

### Acknowledgment

We used the KiK-net seismograms by National Research Institute for Earth Science and Disaster Prevention.

Keywords: moment magnitude, quick estimation, permanent displacement, strong motion record

SSS26-05

Room:304

Time:May 20 10:00-10:15

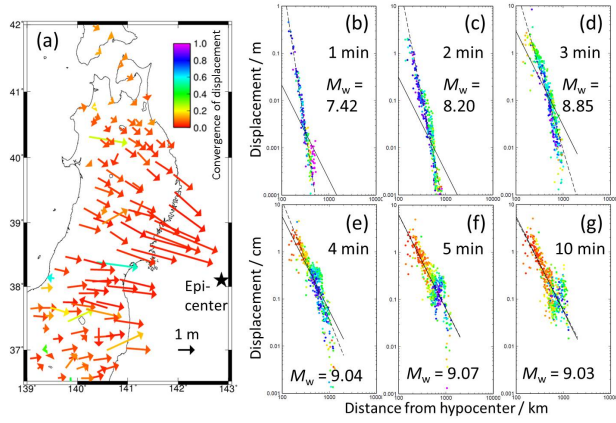


Fig. (a) Permanent displacement distribution. (b)-(g) Real-time magnitude estimation.



## Scaling relations of source parameters for great earthquakes on long active fault systems and plate boundaries

TAJIMA, Reiko<sup>1\*</sup>, Yasuhiro Matsumoto<sup>1</sup>, SI, Hongjun<sup>1</sup>

<sup>1</sup>Kozo Keikaku Engineering Inc.

We investigated seismic scaling relations of rupture area (S), average slip (D), combined area of asperities (Sa) and short-period source spectra (A) versus seismic moment (Mo) for 6 crustal earthquakes with Mw >= 7.5 on long active fault systems and 6 plate-boundary earthquakes with Mw >= 8.4, to examine the validity of the scaling relations derived by past-study, and to understand the difference between source parameters derived from long-period source models with heterogeneous slip and short-period characterized source models. This study is a part of results of the contract study "Comparative study of scaling relations of source parameters for great earthquakes on long active fault systems and plate boundaries" from the Nuclear Safety Commission of Japan.

For the crustal earthquakes we found that the Mo-S relation fits in the line derived by Murotani et al. [2010] which is assuming a proportion to Mo<sup>1</sup> (Figure. 1a). The relationship corresponds to the third stage in 3 stage scaling model [Irikura et al., 2004] which is caused by the saturation of maximum displacement (Dmax) at approximately 10 m. This is also confirmed in our result of the Mo-Dmax relation. The Mo-Sa relation derived from long-period and short-period models are similar to each other. The S-Sa relation seems to fit in the scaling relation suggested by Somerville et al. [1999]. The Mo-A relation is within a scattering of relationship by Dan et al. [2001].

For the plate-boundary earthquakes we found that the Mo-S relation is clearly smaller than that by Murotani et al. (2008) for the M9 events. We also found that the fault widths seem to saturate at approximately 200 km from our results. Then we derived the following new scaling relation S and Mo for great plate-boundary earthquakes with Mw >= 8.4 (Mo >= 4.4 x 10<sup>22</sup> Nm) assuming a proportion to Mo<sup>1/2</sup>:

$$S \text{ (km}^2\text{)} = 5.88 \times 10^{-7} \times Mo^{1/2} \text{ (Nm)} \dots\dots\dots (1).$$

This corresponds to the second stage in the 3 stage scaling model that is caused by the saturation of fault width due to the restriction of the seismogenic layer in the subduction-zone. We also confirmed that D and Dmax are not saturated, i.e. the relation does not arrive at the third stage in the 3 stage scaling model yet. The Mo-Sa and S-Sa relations derived from long-period models fit in the scaling relations suggested by Murotani et al. [2008]. However the Mo-Sa relation derived from short-period models is 2.5 times as small as that of long-period models, and matches the scaling relation by Sato [2010] using the plate-boundary earthquakes. The Mo-A relation is higher than that by Dan et al. [2001] using the crustal earthquakes, but fits in the relation by Sato [2010] using the plate-boundary earthquakes. We think that it is important to accumulate more source models with the different period range because we could discuss about only the 2011 Tohoku earthquake for the plate-boundary earthquake in this study.

Keywords: great earthquake, source parameter, source model, scaling, asperity, rupture area

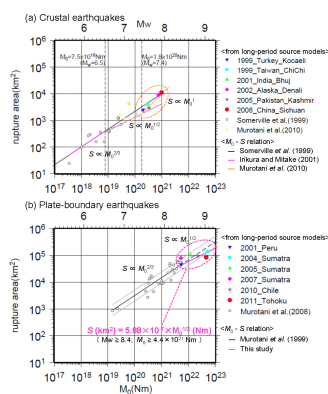


Figure 1. Relation between rupture area (S) and seismic moment (Mo).

## Simulation of strong ground motions from the 2011 Tohoku earthquake and a recipe of predicting strong ground motions for

IRIKURA, Kojiro<sup>1\*</sup>, KURAHASHI, Susumu<sup>1</sup>

<sup>1</sup>Aichi Institute of Technology

### 1. Introduction

Source models of the 11 March 2011 mega-thrust earthquake with Mw 9.0 off the Pacific coast of Tohoku have been investigated by many authors using variety of data-sets from very long-period data such as GPS and Tsunami to short-period data such as teleseismic short period P waves and strong ground motion data. The main slip distributions from very long-period data were located east of the hypocenter toward the Japan Trench zone (Ozawa, et al., 2011 and Fujii and Satake, 2011). A unified source model was constructed through joint inversion of teleseismic, strong motion, and geodetic datasets by Koketsu et al. (2011) and Yokota et al. (2011). They showed that the main rupture propagated not only in the strike direction but also in the dip direction and included both the deep area called the Miyagi-oki region and the compact shallow area near the Japan Trench. On the other hand, we made a source model for generating short-period ground motions comparing observed strong motions with simulated ones using the empirical Green's function method. Our results showed that strong motion generation areas located along the down-dip edge of the source fault. Koper et al. (2011) found the frequency-dependent rupture process of the 2011 Mw 9.0 Tohoku Earthquake comparing source models using backprojection (BP) imaging with teleseismic short-period (<1 s) P waves, and finite faulting models (FFMs) of the seismic moment and slip distributions inverted from broadband (>3 s) teleseismic P waves, Rayleigh waves and regional continuous GPS ground motions. Their results showed indicate that the down-dip environment radiates higher relative levels of short-period radiation than the up-dip regime for this earthquake.

That is, the source models summarized above have common features of the source models that the main slip distributions from the long-period data were located east of the hypocenter toward the Japan Trench zone, while short-period generation areas located west of the hypocenter. These results are not consistent with the basic idea of the recipe of predicting strong ground motions developed based on slip distributions from the waveform inversions for inland crustal earthquake with M 7 class. The recipe was so far constructed based on an idea that large slip areas coincide with strong motion generation area.

In this study, we first summarized source models for generating strong ground motions and then propose an improved idea for recipe of predicting strong ground motions for mega-thrust earthquakes.

### 2. Source models of strong ground motions

We estimate a source model for generating strong ground motions from this earthquake using the characterized source model. Five wave-packets in the observed seismograms were identified, which originated from five strong motion generation areas (SMGAs) on the source fault. The locations of the SMGAs are constrained using the back-propagation method of Kurahashi and Irikura (2010).

Then we obtain the final solutions for the area and initiation point by comparing the observed seismograms of each wave-packet and the synthetic ones at many stations using a trial and error approach. Locations of those five SMGAs seem to correspond to source segments divided for past seismic activity in the region off the Pacific coast of Tohoku by the Headquarters for Earthquake Research Promotion of Japan (HERP). SMGA 1 is located in the source region of Southern Sanriku-oki west of the hypocenter and SMGA 2 in that of the Middle Sanriku-oki north of the hypocenter. SMGA3 is located in the source region of the Miyagi-oki, SMGA 4 is located in that of Fukushima-oki and SMGA 5 is located in that of Ibaraki-oki.

These results suggest a way how to locate such strong motion generation areas for predicting strong ground motions from the mega-thrust earthquake.

### 3. Methodology of predicting strong ground motions for mega-thrust earthquake.

Detailed methodology of predicting strong ground motions is introduced in the session.

Keywords: great earthquake, source parameter, source model, scaling, asperity, rupture area

## Strong motions from the 2007 Niigata-ken Chuetsu-oki earthquake based on characterized source model with super-asperity

SHIBA, Yoshiaki<sup>1\*</sup>, HIKIMA, Kazuhito<sup>2</sup>, UETAKE, Tomiichi<sup>2</sup>, TSUDA, Kenichi<sup>3</sup>, HAYAKAWA, Takashi<sup>3</sup>, Shinya Tanaka<sup>4</sup>

<sup>1</sup>CRIEPI, <sup>2</sup>TEPCO, <sup>3</sup>ORI, <sup>4</sup>TEPCO

Strong motion records of the 2007 Niigata-ken Chuetsu-oki earthquake were obtained at several observation stations in the Kashiwazaki-Kariwa (KK) NPP site. Three distinctive pulse waves are observed in common among these main-shock records, thus they were considered to be radiated from three asperities on the fault plane. On the other hand the observed velocity amplitude of third pulse shows large variation among stations distributing within several hundred meters. Since the base mat of the reactor building where the seismometer is installed is located on bedrock, such variation of observed ground motions cannot be attributed to local site response estimated from shallow subsurface structure. Shiba et al. (2011) calculated the third pulse by using the finite difference method with 3-D deep subsurface velocity model; however the difference of pulse amplitude could not be sufficiently derived by assuming characterized source model. In this study we examine the detailed wave propagation from the asperity generating third pulse (i.e. third asperity) to KK-NPP site by dividing the asperity area into small sub-areas, and find that the variation of third pulse's amplitude becomes apparent when the seismic waves are radiated from only the southwestern part of the asperity. Source inversion analysis simultaneously searching the slip and the peak slip rate also shows locally high slip rate at the southwestern corner of the third asperity. Thus we assume the characterized source model having the super-asperity with relatively high stress drop on the southwestern corner of the third asperity, and carry out the broadband strong-motion simulation at the KK-NPP site. As a result the observed third pulse waveforms for the EW component are successfully reproduced including the quantitative variation. However for the NS component the fit between the observed and the synthetic pulses are insufficient. In the characterized source model the spatial variation of the rake angle on the fault plane is not taken into consideration, and it might cause the different goodness of fit between two horizontal components.

Keywords: the 2007 Niigata-ken Chuetsu-oki earthquake, characterized source model, strong-motion simulation, super-asperity, source inversion

## Revision of seismic hazard assessment after the 2011 Tohoku earthquake

FUJIWARA, Hiroyuki<sup>1\*</sup>, MORIKAWA, Nobuyuki<sup>1</sup>, OKUMURA, Toshihiko<sup>2</sup>

<sup>1</sup>NIED, <sup>2</sup>Shimizu corp.

The Tohoku-oki earthquake (Mw 9.0) of March 11, 2011, was the largest event in the history of Japan. This magnitude 9.0 mega-thrust earthquake initiated approximately 100 km off-shore of Miyagi prefecture and the rupture extended 400 - 500 km along the Pacific plate. Due to the strong ground motions and tsunami associated by this event, approximately twenty thousand people were killed or missing and more than 220 thousands houses and buildings were totally or partially destroyed. This mega-thrust earthquake was not considered in the national seismic hazard maps for Japan that was published by the headquarters for earthquake research promotion of Japan (HERP). By comparing the results of the seismic hazard assessment and observed strong ground motions, we understand that the results of assessment were underestimated in Fukushima prefecture and northern part of Ibaraki prefecture. Its cause primarily lies in that it failed to evaluate the M9.0 mega-thrust earthquake in the long-term evaluation for seismic activities. On the other hand, another cause is that we could not make the functional framework which is prepared for treatment of uncertainty for probabilistic seismic hazard assessment work fully. Based on the lessons learned from this earthquake disaster and the experience that we have engaged in the seismic hazard mapping project of Japan, we consider problems and issues to be resolved for probabilistic seismic hazard assessment and make new proposals to improve probabilistic seismic hazard assessment for Japan.

After the Tohoku-oki earthquake, HERP had been reviewing the long-term evaluation for the area in which the Tohoku-oki earthquake occurred and released the revised version of the "Long-term evaluation of seismic activity for the region from the off Sanriku to the off Boso" in November 2011. In this revision, although the revision of the methodology of the long-term evaluation itself has not yet been made and the most part has remained a traditional evaluation, a new assessment has been made of the Tohoku-oki type earthquake. Based on this evaluation, we have been making a revision of the seismic hazard assessment. In this revision, not only results of the long-term evaluation have been revised, but also the upper limits of background earthquakes have been revised. In addition, here we propose three models in order to consider uncertainty of seismic activity.

We also have prepared the maps that show the strong-motion level for earthquake preparedness. For example, based on the averaged long-term seismic hazard assessment, evaluating strong-motion level for 5,000, 10,000, 50,000, 100,000 years return period, we have made the maps that show the distribution of strong-motion level, which represent effect of major earthquakes on active faults and subduction zone earthquakes with low-probability.

Keywords: National Seismic Hazard Maps, strong-motion, seismic hazard, probability

## Change in site amplification factors before and after the 2011 Off Tohoku earthquake

TAKEMOTO, Teito<sup>1\*</sup>, FURUMURA, Takashi<sup>2</sup>, MAEDA, Takuto<sup>2</sup>

<sup>1</sup>Earthquake Research Institute, the University of Tokyo, <sup>2</sup>Center for Integrated Disaster Information Research, Interfaculty Initiative in Information Studies

### **Introduction**

We have compared between estimated broad band site amplification factor before and after the 2011 Off Tohoku earthquake at each site of the K-NET, KiK-net and F-net strong motion network in Japan. The amplification factors are estimated by coda normalization method (e.g. Phillips and Aki, 1986).

Estimated amplifications are applied for shaking intensity to show the validity of our estimates on the site amplification factors at each site and in frequencies (Takemoto et al., 2012 in press). In this paper, we also found even KiK-net borehole stations have strong site effect.

In this study, we confirmed that site amplification over 4 Hz significantly drops after 2011 Off Tohoku earthquake.

### **Data and Method**

We used KiK-net surface and borehole stations and F-net nation-wide strong motion network developed across Japanese Islands. Using waveform data of acceleration record from 48 moderate earthquakes, we estimated the site amplification characteristic at each station in four frequency bands ( $f = 0.5-1$  Hz,  $1-2$  Hz,  $2-4$  Hz, and  $4-8$  Hz).

The distribution of the site amplification characteristic in each frequency bands has been estimated by inversion. We assumed an F-net broadband seismic observation station installed in the basement rock site as unity (0 dB) site amplification. We also estimate site amplification after 2011 Off Tohoku earthquake using 4 events in northeastern Japan.

### **Results**

In the high-frequency band ( $f = 0.5-1$  Hz), we cannot confirm change of site amplification after the Tohoku earthquake. In the high frequency band ( $4-8$  Hz), site amplification factors in most stations drop around half value.

Site amplification from coda normalization method is value relative to one F-net station. If absolute site amplification in F-net increase, site amplification factor of all stations will drop. For check the change of site amplification without certain reference, we compared two acceleration waveform at FKS006, where site amplification largely drop after Tohoku quake, and FKSH09, where site amplification drop small, in two quakes that location and mechanism are similar each other. Hypocentral distance from two events to stations are almost same. In 2010 event, amplitude at FKS006 is larger than FKSH09 by over seventh. This indicate site amplification in FKS006 is much larger than FKSH09. On the other hand, in 2011 event, amplitude at FKS006 is about twice to FKSH09. Therefore, we can confirm change of the site amplification from waveform. We will estimate the change of site amplification more quantitative in future study.

### **Acknowledgement**

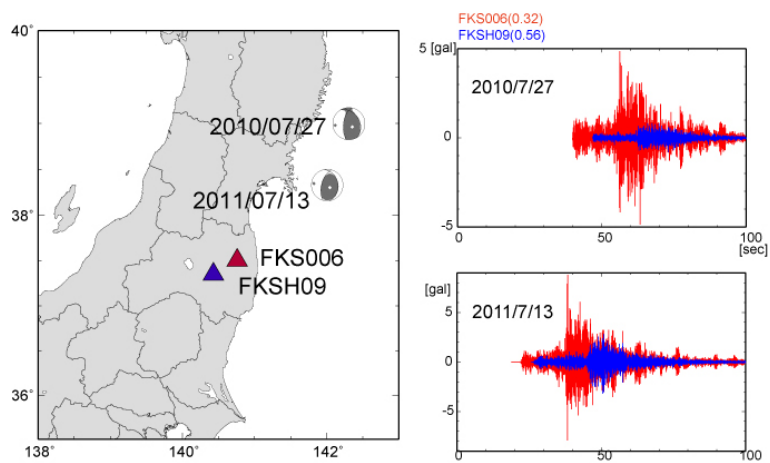
We acknowledge the National Research Institute for Earth Science and Disaster Prevention, Japan (NIED) for providing the K-NET, KiK-net and F-net waveform.

Keywords: 2011 Off Tohoku earthquake, site amplification

SSS26-10

Room:304

Time:May 20 11:45-12:00



## Development of a new ground motion prediction equation applicable up to Mw9 -evaluation of additional correction terms-

MORIKAWA, Nobuyuki<sup>1\*</sup>, FUJIWARA, Hiroyuki<sup>1</sup>

<sup>1</sup>NIED

We have proposed a new ground motion equation in Japan directly applicable up to Mw=9 by using strong motion data of the 2011 Tohoku-oki earthquake. The equation is a simple base model using only two parameters, Mw and closest distance to the source fault. In this study, we obtain following three additional correction terms applied to the above basic equation. The first is the term for amplification due to deep sedimentary layers. We investigate the relation between the amplification and top depth of each layer using the deep subsurface structure model by Fujiwara et al. (2009). The second is the term for amplification due to shallow soil structures using the average S-wave velocity up to 30m depth as a parameter. The third is the term for anomalous seismic intensity distribution using the closest distance from the volcanic front to target site as a parameter.

Keywords: ground motion equation, strong motion, site amplification, anomalous seismic intensity distribution

## Building Damage Ratios and Ground Motion Characteristics during the 2011 off the Pacific coast of Tohoku Earthquake

WU, Hao<sup>1\*</sup>, MASAKI, Kazuaki<sup>2</sup>, IRIKURA, Kojiro<sup>3</sup>, WANG, Xin<sup>3</sup>, KURAHASHI, Susumu<sup>3</sup>

<sup>1</sup>Graduate School of Engineering, Aichi Institute of Technology, <sup>2</sup>Department of Urban Environment, Aichi Institute of Technology, <sup>3</sup>Disaster Prevention Research Center, Aichi Institute of Technology

The relationship between building damage ratios and ground motion characteristics, such as peak ground accelerations (PGAs), peak ground velocities (PGVs), JMA seismic intensities (LJMAS), spectral intensities (SIs), acceleration response spectra (Sa) and pseudo velocity response spectra (pSv) was discussed for the 2011 off the Pacific coast of Tohoku Earthquake. In this study, damage ratio is defined as the ratio of the number of damaged buildings including collapsed, half-collapsed and partially damaged ones, to the total number of buildings in each district (an administrative unit, such as a city, or town). The damage statistics were obtained from the Fire and Disaster Management Agency published on January 13, 2012. The districts mainly damaged by tsunami were excluded. It was found that DRs correlated better with velocity indices such as PGVs, pSv and SIs than acceleration ones such as PGAs, Sa and LJMAS, and DRs correlated better with pSv at 0.5 s than those at 1.0 s and 1.5 s from the view of coherence coefficients. In general, DRs tended to increase with the level of ground motion characteristics, but the damage ratios in some districts did not correspond to suitable level of ground motion characteristics. It was suggested that the ground motion characteristics at the K-NET and KiK-net stations might not represent those in the damaged districts because the stations are far away from the damaged areas.

In order to establish the relationship between building damage ratios and ground motion characteristics in the damaged areas, the estimations of ground motion at the damaged sites were performed based on microtremor measurements. They were accomplished by the product of bedrock motions and site amplification factors at the damaged sites. The ground motions on bedrock under damaged sites and observation stations were assumed to be the same. The bedrock motions under the damaged sites were estimated from observation spectra on surface divided by site amplification factors at the observation station. Then the ground motions were estimated from the product of the bedrock motions and site amplification factors at the damaged sites. Therefore, it was necessary to find the subsurface S-wave velocity structures both at the observation station and damaged site to estimate site amplification factors. Based on one dimensional Haskell multiple reflection theory, the S-wave velocity structures were obtained by inversion of the microtremor H/V spectral ratios. We conducted microtremor measurements and building damage survey at the observation station and the damaged sites. The H/V spectral ratios of microtremor at the observation station showed good consistency with those of ground motions from small earthquakes, which indicated that the inversion of microtremor H/V spectral ratios was feasible, just as the seismic motion ones. The ground motion characteristics at the damaged sites estimated by the above procedure were related with the damage ratios.

Keywords: ground motion characteristics, building damage ratio, S-wave velocity structure, H/V spectral ratio



## Shear-Wave Velocity Evaluation from Microtremor Records Measured in a Damaged Nine-Story SRC Building

WANG, Xin<sup>1\*</sup>, MASAKI, Kazuaki<sup>2</sup>, IRIKURA, Kojiro<sup>1</sup>

<sup>1</sup>Disaster Prevention Research Center, Aichi Institute of Technology, <sup>2</sup>Department of Urban Environment, Aichi Institute of Technology

The building analyzed in this paper is a severely damaged nine-story steel reinforced concrete (SRC) building during the 2011 off the Pacific coast of Tohoku Earthquake, which was designed and constructed in 1990 according to the new anti-seismic design code of Japan. Hereafter it is called K9SRC for short. Obvious shear cracks happened in the external concrete walls in the longitudinal direction (EW), which can be defined as non-structural damage. However, the shear deformation of walls brought about distortion of entrance doors, which hindered escape during the earthquake. The building K9SRC suffered structural damage in the northwest corner column of the first story and multistory shear walls of lower stories, whose steel bars have yielded and been exposed to air. After the earthquake, the building K9SRC was classified to be dangerous. Residents have to move out until it is repaired.

According to the preliminary reconnaissance report of the 2011 Tohoku-Chiho Taiheiyo-Oki Earthquake published by the Architectural Institute of Japan, buildings constructed after 1981 generally showed a good performance during this earthquake, and few of them suffered severe damage. Furthermore, based on the on-site investigation performed by our study group, there are no buildings damaged as severely as the building K9SRC within 1000 km of it. Therefore, the building K9SRC should be paid more attention to scrutinize the damage of it.

In this paper, we made comparative observations of microtremors on each floor and the top of the building K9SRC to extract the shear-wave velocity ( $V_s$ ) traveling within each story using the deconvolution method. Because the shear wave velocity relates only with the seismic property of the structure, it is a reliable way to evaluate the inter-story shear stiffness degradation.

Based on the analyses,  $V_s$  decreases more greatly in the longitudinal direction than in the transverse direction. The interfloor  $V_s$  in the longitudinal direction has decreased to less than 300 m/sec. In the transverse direction, the  $V_s$  decrease along the height of the building, and  $V_s$  traveling in the lower four stories are higher than 300 m/sec.  $V_s$  traveling within the first story decreased obviously because of the damage of the corner column. The  $V_s$  traveling within the 5th and 6th story decreased to less than 300 m/sec in both of the longitudinal and transverse direction.

Keywords: shear-wave velocity of buildings, deconvolution method, microtremor measurement, damaged building

## Continued effort for the Development of the i-Jishin cloud system

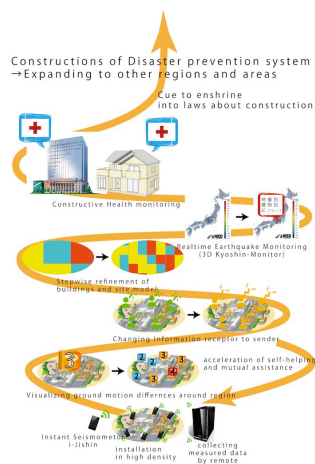
AZUMA, Hiroki<sup>1</sup>, NAITO, Shohei<sup>1\*</sup>, FUKUMOTO, Rui<sup>3</sup>, NAKAMURA, Hiromitsu<sup>1</sup>, SENNA, Shigeki<sup>1</sup>, FUJIWARA, Hiroyuki<sup>1</sup>, YOSHIDA, Minoru<sup>2</sup>

<sup>1</sup>National Research Institute for Earth Science and Disaster Prevention, <sup>2</sup>Hakusan Corporation, <sup>3</sup>Wingbase Inc.

Yoshida et al. (2011) developed an experimental sensor network of earthquake observation using iPhone/iPad/iPod-touch named i-Jishin, and released at App Store in August, 2010.

We introduce after works on this session.

Keywords: i-Jishin, Application, ground motion measurement, cloud, sensor, disaster prevention



## Wave Features Theory of 2011.2NZ Earthquake Motion

NISHIZAWA, Masaru<sup>1\*</sup>

<sup>1</sup>None

### Abstract

Because of Soft Ground Phase of Seismic Wave deviated from correct behavior and generated Rotation around CTV Building.

Keywords: Seismic Wave, Wave Features Theory, Soft Ground, Rotation

## Ishimoto-Iida Law at CEORKA Network

KATO, Mamoru<sup>1\*</sup>

<sup>1</sup>GSHES, Kyoto Univ.

We propose the Ishimoto-Iida law as a statistic tool for a large strong motion waveform database. We demonstrate that the Ishimoto-Iida law is applicable to statistics of PGV at Committee of Earthquake Observation and Research in the Kansai-Area (CEORKA), a velocity-type strong motion network in western Japan.

Amount of strong motion waveforms has increased significantly in the last two decades, which is consequence of recent rapid expansion of observation networks. Such abundance of waveform data enables us to study and understand aspects of the strong motion propagation statistically, the results of which include published attenuation relation formulae and empirical relationship among ground motion parameters such as intensity and PGV or PGA. Here we reevaluate and propose Ishimoto-Iida law [Ishimoto and Iida, 1939] to investigate strong motion statistically. Ishimoto-Iida law expresses relationship between the observed amplitude and total number of observations in any station and time period. Similar to Gutenberg-Richter law (GR law), which expresses the relationship between the magnitude and total number of earthquakes in any given region and time period, Ishimoto-Iida law is a power law. Definition of earthquake magnitude often include amplitude of seismogram as one of the terms, and when GR law governs the seismicity in the area, we would expect that Ishimoto-Iida law holds at stations in that area, at least qualitatively. It is not straightforward to relate GR and Ishimoto-Iida laws quantitatively, and we need to incorporate knowledge of source spectra, propagation and site effects. Investigating Ishimoto-Iida law also provides an opportunity to compare the observed and predicted statistics of the strong motion at particular site under consideration, which could be used to test some aspects of recipe for strong motion prediction.

We used all the strong motion records recorded at CEORKA network between 1993 and 2010 that are tied to JMA earthquake unified catalog. We calculate the horizontal peak ground velocity (PGV) for each record, and analyze the frequency distribution and cumulative frequency distribution of the PGV. When all the observation from the network is combined, the amplitude-frequency diagram has a linear portion in log-log plot, which indicates that the power law, Ishimoto-Iida law, is realized at CEORKA. Amplitude-frequency relations at each station exhibit similar power law, but power in the Ishimoto-Iida law is not a constant within this network.

We model the observed Ishimoto-Iida law using the distance-attenuation relation, the site amplification factor, and the JMA unified hypocenter catalog. Existing attenuation relations are derived from the regression analysis of waveform records of large magnitude events, and we try to use the same relation by extrapolating to smaller events. We used both Shi and Midorikawa [1999] and Kanno *et al.* [2006], but neither relation predicts the observation well. Our current scheme tends to over-predict PGV when the observed PGV is small, and is not successfully predicting observed power of Ishimoto-Iida law.

Keywords: strong motion, seismic wave propagation, site effects

## Characteristics of Seismic Ground Motion in Japan deduced from JMA Intensity Database

Yumi Kohayakawa<sup>1</sup>, KATO, Mamoru<sup>2\*</sup>

<sup>1</sup>IHS, Kyoto Univ., <sup>2</sup>GSHES, Kyoto Univ.

JMA Seismic Intensity is an index of seismic ground motion which is frequently used and reported in the media. While it is always difficult to represent complex ground motion with one index, the fact that it is widely accepted in the society makes the use of JMA Seismic Intensity preferable when seismologists communicate with the public and discuss hazard assessment and risk management. With the introduction on JMA Instrumental Intensity in 1996, the number of seismic intensity observation sites has substantially increased, and the observed data should represent some aspects of the seismic ground motion in Japan. We report our attempt to investigate characteristics of seismic ground motion in the last 50 years utilizing JMA Seismic Intensity Database.

It is empirically known that observations of large intensity is rare compared to those of small intensity. Previous studies, e.g., Ikegami (1961), conclude that frequency distribution of observed intensity obeys the Ishimoto-Iida law (Ishimoto & Iida, 1939). We are able to confirm Ishimoto-Iida law with recent Instrumental Intensity data, but observed number of large intensity is smaller than extrapolated and predicted from those of small intensity. In any calendar year, the average observed number of felt ground motion at any station is approximately 10. At stations with long recording period, there is no apparent difference between pre-instrumental and instrumental intensities when we use Ishimoto-Iida law as a measure.

Numbers of average felt ground motions per year and slopes of intensity-frequency curve are site-dependent and time-dependent. These numbers are strongly affected by the large earthquakes and seismic swarms in the vicinity of the observation site, but the annual change of these parameters appears to be small at all stations. Seismicity at its vicinity controls number of observation at each station.

PGA at observation sites are also listed in Intensity Database. Frequency distribution of PGA also obeys Ishimoto-Iida law. There is no clear linear relationship between Intensity and PGA. In the current formulation of Instrumental Intensity duration of the ground motion is taken into consideration, and this should be the cause of lack of linearity between PGA and intensity.

Keywords: Seismic strong motion, Seismic intensity

## Visualization of strong motion in the 2005 Fukuoka earthquake

FUJIOKA, Akira<sup>1\*</sup>, TAKENAKA, Hiroshi<sup>2</sup>, OKAMOTO, Taro<sup>3</sup>, MURAKOSHI, Takumi<sup>4</sup>, OHSHIMA, Mitsutaka<sup>5</sup>

<sup>1</sup>Faculty of Sciences, Kyushu Univ., <sup>2</sup>Faculty of Sciences, Kyushu Univ., <sup>3</sup>Tokyo Institute of Technology, <sup>4</sup>Dept. of Earth and Ocean Sciences, National Defense Academy, <sup>5</sup>SHIMIZU CORPORATION

Earthquakes occur deep under the ground, so we can observe neither interior of the earth or hypocenter. As is not only the case with earthquakes, it seems natural to use computer simulations to study what out of reach of us. In this paper, we visualize records of the earthquake as part of computer simulations. Here we use records of the 2005 Fukuoka earthquake (Mjma7.0) which occurred on March 20. We used strong-motion records of Fukuoka prefecture, Kyushu University, K-NET and KiK-net (total number of 113). Original records are acceleration except some stations of Kyushu University. We integrate them to the displacement records, and resampled to 10 Hz. We visualize these three-component seismic motions in each direction. We make geographical data with the 250m-mesh Digital Elevation Model supplied by the Geographical Survey Institute. For visualizing we use ParaView.

From the visualization, we can see propagation characteristics of P-wave and S-wave. We can also see opposite polarities of the P-wave across the extension line of fault and propagation of the forward rupture directivity pulse (so-called killer pulse) along the extension of fault. After S-wave passed at some stations, we can see propagation of Rayleigh wave. It also found that seismic motion was amplified in a basin, and there are areas in which attenuation caused by time course was smaller than other areas. There is soft ground in Tsukushi Plain, and seismic waves remained over the long duration there. One minute after the earthquake occurred, they were attenuated in most areas, but in Tsukushi plain, they were still remained.

**Acknowledgments:** We used strong-motion records supplied by Fukuoka prefecture, Kyushu University and the National Institute for Earth Science and Disaster Prevention (K-NET, KiK-net) and 250m mesh Digital Elevation Model published by Geographical Survey Institute.

**Keywords:** visualization, strong motion, 2005 Fukuoka earthquake

## Improvement of Ground Motion Prediction Equation Utilizing Aftershock Records of the 2011 Tohoku Earthquake

TSUTSUMI, Naoko<sup>1\*</sup>, Tatsuya ITOI<sup>2</sup>, Tsuyoshi TAKADA<sup>3</sup>

<sup>1</sup>Graduate Student, the University of Tokyo, <sup>2</sup>Project Assistant Prof., the University of Tokyo, Dr. Eng, <sup>3</sup>Prof., the University of Tokyo, Dr. Eng.

### 1. Introduction

Since the Kobe Earthquake in 1995, dense seismic observation has been deployed all over Japan. Ground motion prediction equations based on the records observed have been proposed, for an intensity measure such as acceleration response spectra. Though it is desirable that site-specific correction should be made, a single coefficient is usually used all over Japan partly because of insufficient number of records at each station, partly because of purpose of prediction applicable for all sites with some explanatory parameters regarding site conditions. Effect from earthquake source mechanism such as fault type should also be considered. Moreover, the uncertainty regarding wave propagation path should be taken into consideration for further improvement of ground motion prediction.

On 11 March 2011, the 2011 off the Pacific coast of Tohoku Earthquake occurred. Thousands of aftershocks occurred within half a year, and ample strong motion records were observed. Since lots of records from thousands of aftershocks occurred in quite wide subduction zones of an epicentral region of the main shock, taken at hundreds of KNET stations in Tohoku region are available in the present, these ample records must be fully utilized for studying effects of site, path and source mechanisms on the ground motion prediction.

In this paper, we correct an existing ground motion prediction equation in order to construct site (or area) specific ground motion prediction model at the Tohoku area, using the aftershock records (inter-plate earthquakes). Two corrections are made; one is the correction associated with site characteristics, and the other is the correction associated with the hypocenter location. The ordinary correction procedure based on statistical minimization of residual is applied for PGA (peak ground acceleration), PGV (peak ground velocity) or Sa (acceleration response spectrum). Then, the standard deviation of residuals is compared both for aftershocks and for past large earthquakes (hereafter, called test earthquakes) occurred in the same rupture zone of 2011 Tohoku Earthquake.

### 2. Results

#### 2.1. PGA and PGV

For aftershocks, both two corrections, i.e. correction for site characteristics and for hypocenter location, improve the prediction accuracy, and the standard deviations decrease. Correction on hypocenter location reduces the standard deviation more than correction on site characteristics does. For test earthquakes, on the other hand, the standard deviation of the case with corrections tends to increase slightly. From this result, it is concluded that it seems to be difficult to apply the correction terms derived from the aftershock records directly to the past earthquakes.

#### 2.2. Acceleration response spectrum

For aftershocks, the standard deviations become small at all periods both for site correction and the hypocenter location correction. For test earthquakes, the standard deviation increases for the shorter period. It is considered because this may come from the effect of the nonlinearity of the subsurface ground. The standard deviations of PGA and PGV are also larger even after site correction made in section 2.1, which may come from the same reason. Standard deviation after hypocenter location correction slightly decreases, though it is not as drastically as that for aftershocks. The possible reasons would be inaccuracy in hypocenter correction term based on spatial interpolation.

### 3. Summary

The correction terms calculated from the observed aftershock records of the 2011 off the Pacific coast of Tohoku Earthquake improve the accuracy of ground motion prediction to some extent for the past strong ground motions. The future work is to improve the accuracy in the short period. It is required that the number of aftershock records increases, effect of the nonlinearity of the subsurface ground is confirmed and the correction regarding hypocenter locations is reexamined.

Keywords: Ground motion prediction equation, aftershock records, site-correction

## Microtremor array survey for subsurface structure of active faults in the 2008 Iwate-Miyagi earthquake source region

KUWAHARA, Yasuto<sup>1\*</sup>, CHO, Ikuo<sup>1</sup>, LING, Suqun<sup>2</sup>, MARUYAMA, Tadashi<sup>1</sup>

<sup>1</sup>AIST, GSI, <sup>2</sup>geo-Analysis Institute Co. Ltd

A microtremor array survey was carried out to depict subsurface structures around a back thrust and a flexure deformation zone in the 2008 Iwate-Miyagi inland earthquake source region. A survey area of Hanokidachi, Ichinoseki city, is characterized by relatively strong inhomogeneous 3D structures, which is not a usual target of a microtremor array survey.

A vertical component seismometer array is composed of two equilateral triangles, one of which has 75 m of a side of the triangle, and the other triangle has 32 m of a side. A total of 11 microtremor survey points were arranged along a 2D line to cover the back thrust and the flexure deformation zone with a survey line length of 500 m. A natural frequency of seismometers used is 0.2 Hz. A total of 60 min data were recorded simultaneously at the seven locations at each array using 24 bits digital recorders with a sampling rate of 100 Hz.

Dispersion curves of the Rayleigh waves were extracted from the vertical component of microtremors using the spatial autocorrelation (SPAC) method (Okada et al. 1987). The dispersion curves were obtained at each array point along the 2D line described earlier. An apparent S-wave velocity profile (Ling et al, 2003) is used to show a cross section of the velocity structure, converted from the Rayleigh wave dispersion curves. An S-wave velocity inversion analysis was also applied at three array points to verify the apparent S-wave velocity structures.

Dispersion curves obtained show generally normal property with phase velocities from 1500 m/s to 500 m/s for a frequency range between 1.2 Hz and 7 Hz, while the dispersion curves for the foot wall side of the back thrust show anomalous behaviors for frequencies over 1.5 Hz. The apparent S-wave velocity profile shows anomalous structures related to the back thrust and the flexure deformation zone. It is noted that the apparent S-wave velocity structures are consistent with the true S-wave velocity structures obtained by the inversion analysis at the three array points.

Keywords: microtremor array survey, active fault, subsurface structure, the 2008 Iwate-Miyagi inland earthquake, back thrust, flexure deformation zone



## Applicability of seismometers JU-215 to shallow-structure explorations using miniature microtremor arrays (<1m)

CHO, Ikuo<sup>1\*</sup>, SENNA, Shigeki<sup>2</sup>, FUJIWARA, Hiroyuki<sup>2</sup>

<sup>1</sup>National Institute of Advanced Industrial Science and Technology, <sup>2</sup>National Research Institute for Earth Science and Disaster Prevention

We have so far shown the possibility to analyze the dispersion characteristics of Rayleigh waves with wavelengths longer than 100 m by observing vertical-component microtremors using a circular array with radius less than 1 m if we are provided with high-performance (low-noise) seismometers (e.g., Cho et al., 2008). A microtremor/strong-motion observation kit JU-215, which was co-developed by the NIED and Hakusan Co. (Senna et al., 2006, 2008), consists of low-noise accelerometers, JA40GA04, manufactured by Japan Aviation Electronics Industry, Ltd (Kunugi et al., 2006) and a recording system with a wide dynamic range 135 dB, DATAMARK LS700XT, manufactured by Hakusan Co. The applicability of JU-215 to the exploration method described above was examined based on observed data in this study.

More concretely, we conducted circular-array observations at 21 sites in and around the Tsukuba city during October to November, 2011. The arrays had radius either 40 cm or 60 cm consisting of six kits of JU-215. We adopted a drawing software, Adobe Illustrator, to draw a real-size array and placed the seismometers directly on the hardcopy in situ (Photo 1). We installed three arrays on earthen roads and eighteen arrays on blacktop roads. The observation durations were 30 minutes with a time interval of 0.01 s. We analyzed the phase velocities of Rayleigh waves by applying either the CCA method (Centerless Circular Array Method; Cho et al., 2004, 2006) or noise-compensated CCA method (Tada et al., 2007) to the vertical-component waveforms. We used a software, microtremor analysis codes BIDO that has been released on the internet via url <http://staff.aist.go.jp/ikuo-chou/bidodl.html>.

As a result, the upper limit of the wavelength range analyzable was 160 m at the maximum and about 100 m on average. This means that the maximum wavelengths relative to the array radius get a few hundred at the maximum and 170 on average. The SN ratios that were separately analyzed in this study took values about 10,000 in the frequency ranges between 2 to 10 Hz for most sites, being consistent with the analyzable wavelength ranges when we consider the relationship between SN ratios and the maximum wavelengths analyzable by the CCA method (Cho et al., 2006). The SN ratios for the arrays with radii less than 1 m can almost be considered to indicate those for the recording system, validating the high performance of JU-215. The observation kit JU-215 might be able to apply a circular array of four points: one at the center point and three around the circumference, instead of six points. The examination will be done in the future.

We extracted from the analysis results the phase velocities corresponding to the wavelength 40 m regarding them to be AVS30 following Konno and Kataoka (2000). They ranged between 140 to 280 m/s being comparatively well consistent with those deduced from the geomorphologic data (Matsuoka et al., 2005). By adopting miniature-array analyses described here we are able to obtain phase velocities of Rayleigh waves in the frequency ranges from 2-3 Hz to several tens of Hertz, which can be used for more detailed explorations of either shallower or deeper portions of substructures.

Senna, S., S. Adachi, H. Ando, T. Arai, K. Iisawa, H. Fujiwara: Development of microtremor survey observation system, Program of the 115 SEGJ (Society of exploration geophysics of Japan) Conference, 120-122, 2006.

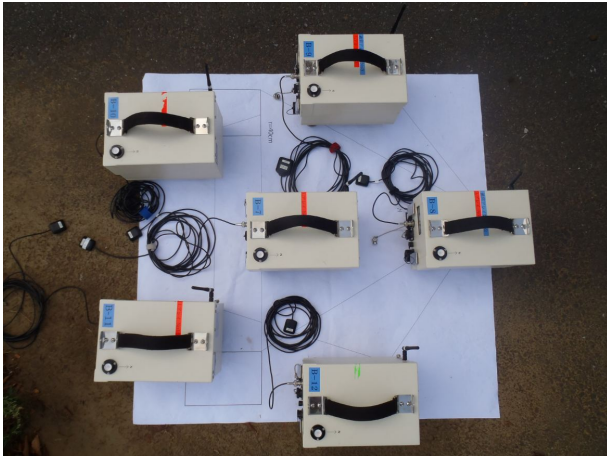
Senna, S. and H. Fujiwara: Development of analyzing tools for microtremor survey observation data, Vol. 1: Tools for analysis of microtremor data, Technical note of the national research institute for earth science and disaster prevention, No. 313, 2008.

Keywords: microtremors, exploration methods, surface waves, phase velocity, velocity structure, AVS30

SSS26-P07

Room:Convention Hall

Time:May 20 17:15-18:30



## Explorations of S-wave velocity structure around the Chikushi plain

OKUDAIRA, Ryota<sup>1</sup>, YAMADA, Nobuyuki<sup>2\*</sup>, TAKENAKA, Hiroshi<sup>1</sup>

<sup>1</sup>Kyushu University, <sup>2</sup>Fukuoka University of Education

We conducted microtremor array measurements for the 5 sites around the Chikushi plain to estimate 1D S-wave velocity profiles of deep sedimentary layers over the basement with a  $V_s$  about 3.0km/s. In this presentation, we will discuss the details of the observation and analysis. We will analyze the data and get the S-wave velocity profiles at the 5 sites. And we will discuss to construct of 3D basin model.

Keywords: Chikushi plain, S-wave velocity structure, microtremor array exploration

## S-wave velocity structure of southern Niigata estimated with ambient noise array surveys

YOSHIMI, Masayuki<sup>1\*</sup>, HAYASHIDA, Takumi<sup>1</sup>, SUGIYAMA Takashi<sup>2</sup>, SAOMOTO, Hidetaka<sup>1</sup>

<sup>1</sup>Geological Survey of Japan, AIST, <sup>2</sup>Chuo Kaihatsu Corp.

We conducted ambient noise array survey in active fold area in Niigata prefecture, Japan, to estimate subsurface S-wave velocity structure. Thirteen noise arrays each with 12 temporal velocity seismometer stations have been set in the area spreading 50 km x 15 km. Each array is an equilateral arrays whose radii ranges from several hundred meters to several kilometers. Each observation is carried out for more than 10 days to assure reliable survey, since the survey needs statistically enough data. Velocity seismometers with natural period more than 5 sec. are deployed connected with 24bit A/D, GPS time-calibrated data loggers to obtain continuous noise data. Each continuous data are segmented to hourly data sets, and are analyzed with SPAC method and V method (Tada et al,2007) to estimate phase velocity using BIDO 2.0 software (Tada et al, 2010,<http://staff.aist.go.jp/ikuo-chou>). In addition, the ambient noise interferometry for surface waves is applied for the data of some stations to estimate group velocities. We successfully obtained phase velocities in the frequency 0.13 to 1.0 Hz, but with large fluctuation at the frequency lower than 0.2 Hz that seemed to be influenced by weather condition.

This research is funded and supported by Japan Nuclear Energy Safety Organization (JNES).

Keywords: sedimentary basin, SPAC method, S-wave velocity structure, Niigata, microtremor, ambient noise

## S-wave velocity structure of southern Osaka plain estimated from ambient noise array survey and H/V spectra

YOSHIMI, Masayuki<sup>1\*</sup>, SEKIGUCHI Haruko<sup>2</sup>, ASANO Kimiyuki<sup>2</sup>

<sup>1</sup>Geological Survey of Japan, AIST, <sup>2</sup>DPRI, Kyoto Univ.

We conducted ambient noise array survey at two locations in southern Osaka plain using 4 velocity seismometers arranged to equilateral array. Applying SPAC and E-SPAC method to the observed data, we estimate phase velocities (dispersion curves). Then, S-wave velocity structures satisfying the dispersion curves are searched using GA method, assuming three layers ( $V_s=0.35, 0.55, 1.0$  km/s) or gradually increasing velocity structure overlaying seismic bedrock ( $v_s=3.2$ km/s). Then analytical H/V has been compared with measurement for validation.

This research is funded by the Comprehensive Research on the Uemachi Fault Zone (in FY2011) by MEXT.

Keywords: SPAC method, sedimentary basin, Osaka, microtremor, ambient noise, H/V

## Relationship between microtremor H/V spectral ratios and basin structure model in the Osaka sedimentary basin

ASANO, Kimiyuki<sup>1\*</sup>, IWATA, Tomotaka<sup>1</sup>, SEKIGUCHI, Haruko<sup>1</sup>, MIYAKOSHI, Ken<sup>2</sup>, NISHIMURA, Toshimitsu<sup>2</sup>

<sup>1</sup>Disaster Prevention Research Institute, Kyoto University, <sup>2</sup>Geo-Research Institute

The Osaka sedimentary basin is filled by the Pleistocene Osaka group and the Quaternary sediments with thickness of 1 to 2 km over the bedrock, and it is surrounded by the Arima-Takatsuki Tectonic Line and the Ikoma active fault system. The Uemachi active fault system underlies the Osaka urban area. In order to predict the strong ground motions from a future event of the Uemachi fault, the precise underground velocity structure model is indispensable as well as the detailed source fault model (e.g., Iwata *et al.*, 2012, this meeting). The underground velocity structure of the Osaka sedimentary basin has been well investigated by using techniques such as gravity anomaly measurements, refraction surveys, seismic reflection surveys, boring explorations, and microtremor measurements. Based on these surveys and ground motion simulations, the three-dimensional basin velocity structure models of the Osaka basin have been developed and improved for decades (e.g., Kagawa *et al.*, 1993; Horikawa *et al.*, 2003; Iwata *et al.*, 2008; Iwaki and Iwata, 2011). In the present study, we conducted microtremor measurements in and around the Osaka basin, and obtained H/V spectral ratios of microtremor in order to contribute to the further improvement of the three-dimensional basin structure model.

The microtremor measurements are conducted from August to December, 2011 at one hundred strong motion stations in and around the Osaka basin. These stations consists seventy-three stations belong to the seismic intensity observation network of the Osaka prefecture, 9 JMA, 11 K-NET, 5 KiK-net, one BRI, and one PARI stations. We measured microtremor at each site more than 30 minutes using the Lennartz velocity sensor LE-3D/20s and the 24bit A/D data logger LS-7000XT. The target period range of this measurement is up to 10 s. We selected more than 10 segments with duration of 81.92 s by eliminating non-stationary noise, calculated their Fourier amplitude spectra, and obtained the ensemble average of the horizontal-to-vertical (H/V) spectral ratios. We identified the dominant periods of the H/V spectral ratios. The dominant periods of the H/V spectral ratios are e.g. approximately 7s around the Osaka port and 3-4 s on the Uemachi platform.

We referred to two three-dimensional basin velocity structure models in Osaka by Iwata *et al.* (2008) and Horikawa *et al.* (2003). The sites with deeper sediments have tendency to show longer dominant periods as partly reported previously by Miyakoshi *et al.* (1997). We extract one-dimensional velocity structure model beneath each site from the original three-dimensional structure models, and calculate the theoretical ellipticity of the Rayleigh-wave. We regard the peak period of the ellipticity as a theoretical dominant period of the H/V spectral ratio for that model. For most stations, theoretical dominant periods agree well to those of the observed H/V spectral ratios. However, the theoretical H/V spectral ratios have longer dominant periods than the observed microtremor H/V spectral ratios at some station in the footwall side of northern part of the Uemachi fault system and Senboku and Habikino Hills. Some sites in Minoh and Shijonawate cities located close to the basin edge where bedrock depth changes steeply. It might be due to inappropriate setting of bedrock depth or three-dimensional wave propagation effects. We will make further analysis to solve them.

Acknowledgements: This research is funded by the Comprehensive Research on the Uemachi Fault Zone by MEXT. We would like to acknowledge Osaka prefecture government, local government offices, JMA Osaka District Meteorological Observatory, Osaka Regional Civil Aviation Bureau, and NIED.

Keywords: Osaka sedimentary basin, microtremor, H/V spectral ratio, basin velocity structure model, dominant period

## H/V spectral analysis of micro-tremor in Kochi Plain

OISHI, Yusuke<sup>1\*</sup>, KUBO, Atsuki<sup>2</sup>, YAMASHINA, Tadashi<sup>2</sup>

<sup>1</sup>Faculty of Science, Kochi Univ., <sup>2</sup>Kochi Earthq. Obs., Fac. of Sci., Kochi Univ.

Kochi is located around source region of the Nankai Earthquake. Soil/basement structure is important to estimate strong ground motion. Modeling the soil/basement structure conducted based on boring core database. In this study, we conducted micro-tremor H/V spectral analysis in Kochi Plain. This technique is cheap, quick and easy way to study soil/basement structure. We observed at 250 points in a year in addition to previous 130 points. Dominant periods of H/V spectra show about 1 sec around Urado-Bay region. Thicker soft ground causes strong ground motion in this region. Generally dominant period is correlated to thickness of Alluvium layer. However, we sometimes detect dominant period variation caused by deeper structure. By detail observations at recognized steep variation of basement, we detect corresponding variation of dominant periods. Spectral peaks with around 1sec periods widely appear in Kochi Plain. Spectral shapes are determined by this peak and higher modes, spectral shape due to Alluvium layer, and more complicated structure.

Keywords: Soil/Basement Structure, H/V spectra, Strong Motion, Kochi Plain, Dominant period

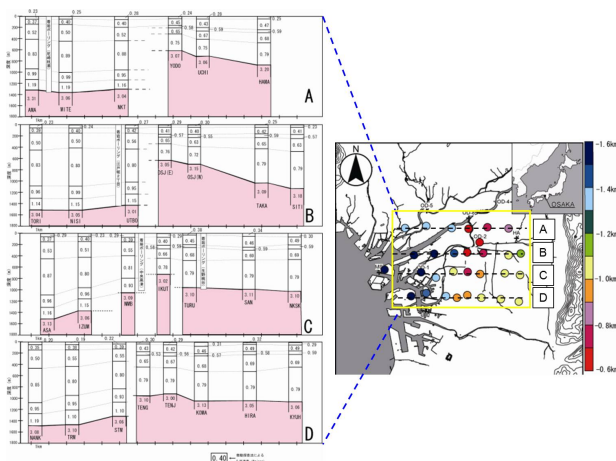
## Deep S-wave Velocity Structure in Osaka Plains Urban Area Estimated by Microtremor Survey Method

MINAMI, Yuichiro<sup>1\*</sup>, MATSUOKA, Tatsuro<sup>3</sup>, MIZUOCHI, Yukihiro<sup>2</sup>, HARAGUCHI, Tsuyoshi<sup>1</sup>

<sup>1</sup>Graduate School of Sci.,Osaka City Univ., <sup>2</sup>Sumiko Resources Exploration & Development Co.,Ltd, <sup>3</sup>Geo-X Consultants Co.Ltd.

In order to investigate the S-wave velocity structures under the Osaka Plain, we carried out long-period microtremor array observations at total 30 sites. Which are covering all of Osaka City area. wiht having the east-west transect line across the Uemachi fault. Phase velocities of the fundamental-mode Rayleigh wave in microtremors were obtained by the spatial autocorrelation method and converted to the S-wave velocity structures by using an inversion technique based on the genetic algorithm (GA). The estimated S-wave velocity structures were in agreed with geological structures which were identified by both the observation of the deep wells and seismic reflection profiles. We could indicate that the S-wave velocity structures provide the obvious difference of the upper level of the basement rock between the west-and the east-side along the in Uemachi fault.

Keywords: microtremor, SPAC, Uemachi fault, deep S-wave velocity





## Seismic interferometry using dense seismic network data in south Niigata Prefecture, Japan

HAYASHIDA, Takumi<sup>1\*</sup>, YOSHIMI, Masayuki<sup>1</sup>

<sup>1</sup>Active Fault and Earthquake Research Center, AIST, GSJ

We applied seismic interferometry to the data recorded by 15 seismic stations in south Niigata prefecture to estimate surface-wave group velocity between selected station pairs. 14 of the 15 stations each have one three-component broadband velocity seismometer (VSE-355JE by Tokyo Sokushin Co., Ltd.) at a depth of 5 m and the other has one seismometer (VSE-355EI) on the ground surface. The average distance between stations is 7.1 km and therefore the analysis makes it possible to evaluate detailed velocity structure in this region and to estimate group velocity in the higher frequency range (0.5-1 Hz). First we computed cross-correlation functions (CCFs) of long-term ambient noise at selected pairs of stations; (a) between all 14 stations and station GYK03 (Niigata Institute of Technology), (b) between stations on three northwest-southeast lines (31 pairs), and (c) between neighboring stations (35 pairs). Here we used 1 hour continuous data for the calculation, after the one bit normalization (Sabra et al., 2005). The shortest and longest distances between the pairs are 4.2 km (GYK04-GYK05) and 40.7 km (GYK01-GYK15), respectively. The stacked CCFs of ambient noise showed coherent and dispersive wave-trains in a wide frequency range (0.05-1.0 Hz). Especially, time-symmetric CCFs were derived in a frequency range between 0.01 and 0.25 Hz. On the other hand, asymmetric CCFs were clearly seen in the higher (0.5-1.0 Hz) and lower (0.05-0.125 Hz) frequencies. Next we compared observed group velocities with theoretically derived dispersion curves near the stations based on a seismic velocity structure model of the Niigata region (Sekiguchi et al., 2009). Observed group velocities correspond well to the dispersion curve at some stations pairs, while the agreements tend to be poor for station pairs where S/N value of the stacked cross-correlation function is low or where the velocity structure is spatially varying between the stations. Continued data acquisition and analysis is important to obtain more stable CCFs and to evaluate the effect of spatial structure change on the group velocity dispersions.

### Acknowledgements;

This research is funded and supported by Japan Nuclear Energy Safety Organization (JNES).

Keywords: seismic interferometry, ambient noise, surface wave, velocity structure model, south Niigata Pref.

## Receiver function analysis for the Osaka plain, southwestern Japan

HORIKAWA, Haruo<sup>1\*</sup>

<sup>1</sup>Active Fault and Earthquake Res. Ctr., AIST/GSJ

Receiver functions are calculated for stations within the Osaka sedimentary basin, southwestern Japan. The calculation was begun with verification of the azimuth of the horizontal components of the seismometers used in this study. The verification was performed with calculating cross-correlation of filtered observed ground motions between stations with in-situ measurement of the azimuth and those without the measurement. It was suggested that the actual direction was different from the assigned one by tens of degrees for several stations. Receiver function then were calculated after Soda et al. (2001) and with the correction of the azimuth of the horizontal components as suggested above. The receiver functions often contain distinct P->S converted phase that is responsible for high impedance contrast at the basin floor, which is the boundary between Pliocene sediment (Osaka Group) and pre-Tertiary rock. The arrival time of the distinct phase in the receiver function is equal to the travel time difference between S-wave and P-wave within the sediment. The observed travel time differences were compared with those calculated from the J-SHIS model developed by the NIED. It was found that the calculated travel differences were often shorter than the observed ones for stations near the northern and eastern basin edges. This shortage comes from parameterization of the basin floor. The J-SHIS model used spline functions for expressing the shape of the basin floor, which made the modeled basin floor smooth. On the other hand, several geophysical explorations revealed that the actual basin floor stays at a depth of around 1 km even at the northern and eastern edges of the basin, and is exposed to the ground surface in a step-wise form. Since the basin edge heavily controls the location of destructive strong motions near a causative fault (Kawase, 1996), parameterization of a basin floor should be further examined.

Acknowledgement: I used ground motion records provided by the CEORKA, NIED (K-Net, KiK-Net and F-Net), and Osaka Prefecture. Tomotaka Iwata and Kimiyuki Asano arranged the use of the Osaka Prefecture's records. Asako Iwaki kindly provided her unpublished results of inference of the azimuth of the seismometers with information on her analysis. This research was supported by the fund of the Comprehensive Research on the Uemachi Fault Zone by MEXT.

Keywords: receiver function, Osaka sedimentary basin, subsurface velocity structure

## Relation between spectral amplitudes of microtremors and maximum seismic amplitudes

TANAKA, Torao<sup>1\*</sup>, OKUBO, Makoto<sup>1</sup>, AOKI, harumi<sup>1</sup>

<sup>1</sup>TRIES

It is important for mitigation of the seismic hazards to investigate the frequency characteristics of oscillations caused by the shallow ground soil structure. If the peak of spectral amplitudes of microtremors is related definitely to that of seismic oscillations, microtremor observations will give us useful information about the spectral peak amplitude of seismic oscillations. Here we calculate the spectral amplitudes of the microtremors and two seismograms observed at three seismic stations at TRIES high density seismographic network by the discrete Fourier transform. The frequency range from 2 to 4Hz is especially important, since many two storied wooden houses are very popular in Japan. We divide the frequency range from 1.95 to 4.04 Hz into 21 intervals of 0.1Hz, decide the minimum spectral amplitudes from 20 or 30 microtremor data, and consider the minimum amplitudes as those under an imaginary quiet circumstances. The maximum spectral amplitude of seismograms is influenced by not only the site effect, but the magnitude, source mechanism, propagation path and so on. In order to avoid the factors except site effect, we use two relative microtremor minimum amplitudes and two relative seismic spectral ratios to those at TRIES, the reference point. Results obtained from the comparison of two earthquakes show nearly parallel distributions to spectral features which correspond to the differences of recorded amplitudes. The peak value frequency of the minimum amplitudes of microtremors will correspond with the characteristic oscillation frequency of the ground soil. This means that the microtremor spectral amplitudes will successfully be used to estimate the maximum spectral amplitudes of earthquakes in the future.

Keywords: microtremor, seismic wave, ground soil, discrete Fourier transform, maximum amplitude, seismic hazard

## Synthesis of high-frequency ground motion based on information extracted from low-frequency ground motion

IWAKI, Asako<sup>1\*</sup>, FUJIWARA, Hiroyuki<sup>1</sup>

<sup>1</sup>NIED

### 1. Introduction

Broad-band ground motion computation of a scenario earthquake is generally based on the hybrid method that is the combination of deterministic approach in lower-frequency band and stochastic approach in higher-frequency band.

In the hybrid method, the low- and high-frequency (LF and HF, respectively) wave fields are generated through two different methods that are completely independent of each other, and are combined at the matching frequency. However, LF and HF wave fields are essentially not independent as long as they are from the same event. In this study, we focus on the relation among acceleration envelopes at different frequency bands, and attempt to synthesize HF ground motion using the information extracted from LF ground motion, aiming to propose a new method for broad-band ground motion prediction.

### 2. Method

Our study area is Kanto area. We use KiK-net borehole acceleration data and compute RMS envelope at four frequency bands: i) 0.5-1.0 Hz, ii) 1.0-2.0 Hz, iii) 2.0-4.0 Hz, iv) 4.0-8.0 Hz. Taking the ratio of the envelopes of adjacent bands, we find that the envelope ratios have stable shapes at each site. We use the envelope ratios as the empirical envelope-ratio characteristics to be combined with low-frequency envelope and random phase to synthesize HF ground motion. We have applied the method to M5-class earthquakes that occurred in the vicinity of Kanto area and successfully reproduced the observed HF ground motion (2011 SSJ Fall Meeting).

### 3. Toward ground motion prediction of M7-class earthquakes

We examine the application of the method for ground motion synthesis of M7-class earthquakes by analyzing interplate and intraslab earthquakes that occurred in the off Ibaraki prefecture region ( $M_{JMA}$  from 5.1 to 7.0) and northern Miyagi prefecture region ( $M_{JMA}$  from 4.5 to 7.0), respectively.

For the interplate earthquakes, the LF envelopes are rich in later-phases while HF envelopes show rapid attenuation that follows the S-wave strong motion part. The rates of attenuation of the envelope ratios show dependency on seismic moment; HF ground motion of a M7-class earthquake shows greater attenuation with respect to LF ground motion relative to M5-class earthquakes. It reflects long-period ground motion generated in both the source process and the propagation path, which is characteristic of large interplate earthquakes. Such dependency on seismic moment is not seen in the intraslab earthquakes. Magnitude-dependent envelope ratios should be modeled in order to be applied to M7-class ground motion prediction.

Keywords: broad-band ground motion prediction

## Estimation of three-dimensional layer interface topography of subsurface structure using a MCMC method

IWAKI, Asako<sup>1\*</sup>, AOI, Shin<sup>1</sup>

<sup>1</sup>NIED

The deep sedimentary structure has strong influence on long-period ground motion. Waveform inversion is an effective way to construct the deep subsurface structure that can reproduce the observed seismic waveform. A waveform inversion method for estimating three-dimensional (3D) layer interfaces of sedimentary basins was proposed by Aoi (2002), in which the inverse problem is quasi-linearized on the assumption of weak nonlinearity between the data and model. The method was applied to real seismic data by Iwaki and Iwata (2011), which suggested its high potential for practical uses. One of the major difficulties of the inversion method is the nonuniqueness of the solution that is inevitable in such optimization procedures, which can cause problems such as strong dependency on the initial model and failure of convergence.

In this study, we formulate the basin topography waveform inversion using a Monte Carlo method. Instead of searching for one best-fitting model by quasi-linearized inversion, we take a global optimization process using a Markov Chain Monte Carlo (MCMC) method, in which the statistical characteristics of the sampled model parameters can be analyzed by Bayesian approach.

We perform a numerical test to investigate the applicability of MCMC method to be used in construction of the deep subsurface structure models. The target model is a 3D basin model with irregular boundary shape whose size is 25 km x 20 km and the maximum bedrock depth is 2500 m. The change in bedrock depth with respect to the initial value is the model parameters to be estimated in this inverse problem. The period range of the analysis is 3-10 sec. The search range is from -400 to 2200 m at 200 m intervals. The basin boundary shape is described by cosine basins functions with 35 nodes; therefore there are  $14^{*}35$  possible models in the model space. In MCMC method, the probability density function (PDF) of the objective function is sampled from the model space by the accept-rejection sampling of the Metropolis-Hastings algorithm. After 9000 trials, we took the mean and standard deviation of the accepted model parameters. The obtained mean model is sufficiently similar to the target model within the resolution of the basins function. It is suggested that global search based on MCMC method is applicable to construction of deep subsurface structure models. It can be combined with the local search, such as the quasi-linearized waveform inversion, especially when there is poor information on initial structure model.

Keywords: subsurface structure, inverse problem, Monte Carlo method

## Vibration test of the seismometer using mobile information terminal on the 3-D Full-Scale Earthquake Testing Facility

NAITO, Shohei<sup>1\*</sup>, AZUMA, Hiroki<sup>1</sup>, SENNA, Shigeki<sup>1</sup>, Mutsuhiro Yoshizawa<sup>1</sup>, NAKAMURA, Hiromitsu<sup>1</sup>, FUJIWARA, Hiroyuki<sup>1</sup>, Yoichi Tanaka<sup>2</sup>, YOSHIDA, Minoru<sup>2</sup>

<sup>1</sup>National Research Institute for Earth Science and Disaster Prevention, <sup>2</sup>Hakusan Corporation

A MEMS(Micro Electro Mechanical Systems) acceleration sensor is commonly used on many mobile terminal devices such as smartphone, personal stereo, and tablet PC, because it is compact, lightweight, and cheap. If we use MEMS sensors to make observations of strong motion, we could know more detailed information of damaged area, and send more rapidly realtime earthquake information.

Yoshida et al. (2011) developed an experimental sensor network of earthquake observation using iPhone/iPad/iPod-touch named "i-Jishin", and released at App Store in August, 2010.

Naito et al. (2011) installed "i-Jishin" on the base and observed in parallel with K-NET02 seismometer. They compared same seismic waves, and concluded over 3 regarding JMA-shindo fit within the margin of 0.1, but up to 2 it becomes overestimate.

To confirm if it have a performance that applies for strong motion observation, we set up 12 machines of iPod-touches on the E-Defense, and observed 10 different kind of seismic waves and white noises.

We fixed iPod-touches on the floor, wall, and desks using adhesive double coated tape. And we charged energy with an external battery, corrected time with an NTP server.

As a result, we acquired all data that was exceeded the trigger level. And the data was comparable to servo type accelerator on the same floor.

The response spectrum showed nonlinear characteristics depending on vibration levels and layers when it shook at strong motion such as JMA Kobe.

Recorded data has some differences depending on a location setting. When we set "i-Jishin" we must set on the floor or on the wall tightly, and be careful not to conflict with surroundings.

On another time, We have made a vibration test on the shaking table and examined in parallel with other standard seismometer. At next time, we will release detail about this examination.

We are aiming to examine a performance of "i-Jishin" as a seismometer in detail, and going to conduct demonstration experiments of cloud MEMS sensor network.

Keywords: MEMS, Sensor Network, Cloud, mobile terminal, i-Jishin, E-Defense

## Construction of the cloud type microtremor observation system

SENNA, Shigeki<sup>1\*</sup>, Hiroki Azuma<sup>1</sup>, Shigeki Adachi<sup>2</sup>, Yuta Asaka<sup>3</sup>, Hiroyuki Fujiwara<sup>1</sup>

<sup>1</sup>NIED, <sup>2</sup>Hakusan Corporation, <sup>3</sup>MSS

The microtremor observation has treated till today as physical investigation information, including the structure model creation for strong motion prediction of the researcher and engineer, etc.

If microtremor observation can observe easily and the observed data can be easily transmitted to a database with information on that observation point, it can expect that the number of collection of observational data will increase explosively in the future because an amateur can also observe, and the advancement of structural model and prediction of seismic strong motions will be attained by leaps and bounds.

It will become an unprecedented thing which leads to grasp of detailed damage distribution, and the improvement in accuracy of real-time earthquake information from the above.

It became somewhat easy to treat microtremor observation now.

However, about the process of the whole microtremor observation, beginners cannot always carry out easily.

We have released battery, sensor and logger integral-type microtremor meter JU-210 which can be observed, and JU-215 (with a Wireless local access network (WLAN)) which an amateur can treat was made.

Moreover, in a senna and Fujiwara (2008), the software which can analyze microtremor data easily is also created and exhibited.

In response to the above-mentioned development, "i-bidou" system which can be observed only with a microtremor meter and a smart phone was built by this research using the smart phone which has spread through a world explosively.

Moreover, about the microtremor meter, JU-310 which improved the communications system etc. was developed so that cooperation with "i-bidou" system could be smoothly taken as an upgrade version of above-mentioned JU-215.

After registration is performed in a microtremor database, it is analyzed automatically.

Moreover, a series of flows which can peruse an analysis result immediately were also built.

It is expected that it will be sharply improved by the tuning time of a structural model according to the Cloud environment from now on. Furthermore, the benchmark test was done by the amateur and was able to obtain the good result.

The future still more user-friendly "i-bidou" system will be built.

Furthermore, correction analysis of the structure model registered into J-SHIS etc., may be able to be conducted at high speed.

Keywords: Microtremor observation, Cloud, Mobile terminal, i-Bidou, Structure, Strong motion prediction

## Development of simple and handy seismometer (SPOT seismometer)

ITO, yoshiaki<sup>1\*</sup>, KORENAGA, Masahiro<sup>1</sup>, YAMAMOTO, Shunroku<sup>1</sup>, NODA, Shunta<sup>1</sup>, IWATA, Naoyasu<sup>1</sup>, Noboru Yuki<sup>2</sup>

<sup>1</sup>Railway Technical Research Institute, <sup>2</sup>Hakusan Corporation

We developed a simple and handy seismometer (SPOT seismometer; Sensor Pod of Train system). A SPOT seismometer mainly consists of a measurement part, a communication processing part, a mobile communication device and a GPS module. It's very compact and lightweight, so as to carry and install it easily. By installing them between permanent stations along rails, we can obtain spatial distribution of ground motions more densely, and use these information for train operation control after earthquakes. It works continuously about more than one month by four D size batteries. The measurement part is equipped with a MEMS accelerometer having the ability to measure seismic shakings correctly in the case of seismic intensity 3 and larger. A SPOT has functions of calculating instrumental seismic intensity and JRPGA (PGA passed 5Hz high cut filter), transmitting calculated seismic parameters and waveform data to a Web server via mobile telephone network when a seismic shaking exceeds a pre-defined threshold. The transmitted information is able to be viewed on website. Simultaneous observation of natural earthquakes by the SPOT seismometer and a seismic intensity meter is carried out and a proper operation of the SPOT is confirmed. In the next step, we plan to verify reliability by continuous operation in the actual environment of railways, and to spread the SPOT seismometer.

Keywords: seismometer, MEMS, train operation control



## Dynamic Analysis of Earthquake Amplification Effect of Slopes in Different Topographic and Geological Conditions

MITANI, Yasuhiro<sup>1\*</sup>, Wang Fawu<sup>1</sup>

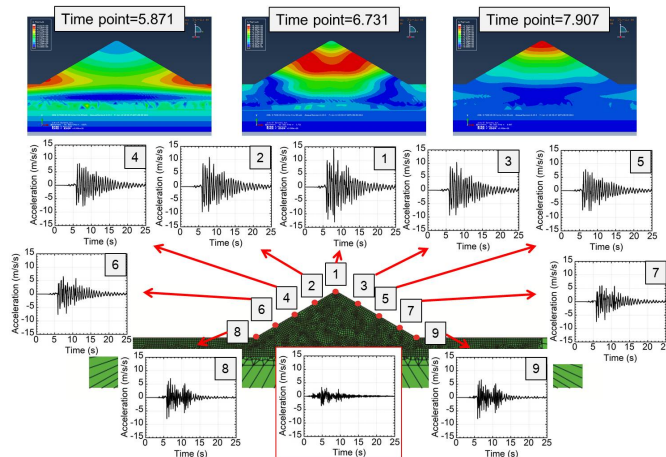
<sup>1</sup>Shimane University Department of Geoscience

Slope failure is always triggered by earthquake, and brings damage to society. In dynamic analysis of slope stability considering the seismic loading, it is important to understand the amplification effect of slope due to topographic and geological structure. However, because the effect processes due to topographic and geological structure are too complicated, the amplification effects are not clear. In this study, an attempt using Abaqus, a FEM software, to clarify the amplification effects is conducted.

At first, infinite element is adopted in the boundary condition. Result of a example slope model is verified by a published centrifuge test result. Analysis has been conducted on the amplification effect for a homogeneous slope due to different height, angle, seismic wave, and dip angle of alternating layers of tuff and shale. Finally, the amplification effects of south-north direction slope and east-west direction slope around the Shimane nuclear power plant (Shimane-NCPP) have also been analyzed.

In this study, amplification factor is defined as the ratio of output peak acceleration to the input acceleration. As the result, (1) at slope top and middle, amplification factor becomes smaller when the slope height becoming larger; (2) amplification factor of slope top becomes relatively bigger when the slope angle becoming larger, however amplification factor of slope foot becomes relatively smaller; (3) amplification tendency does not show obvious difference for seismic wave and dip angle of strata layer; (4) south-north direction slope around the Shimane-NCPP shows high amplification factor near slope top, while east-west direction slope around the Shimane-NCPP shows high amplification factor near slope foot.

Keywords: Abaqus software, amplification effect, infinite element, earthquake, slope failure



## Modeling 3-D subsurface structure for strong ground motion estimation the in Tottori plain

ISHIDA, Yusuke<sup>1\*</sup>, NOGUCHI, Tatsuya<sup>1</sup>, KAGAWA, Takao<sup>1</sup>

<sup>1</sup>Tottori University Graduate School of Engineering

This study was performed for the purpose of constructing 3-D subsurface structure model for strong ground motion estimation in the Tottori plain. First, previously proposed layered structure models were integrated into an averaged layered structure model. Thickness of each layer was estimated at microtremor array observation site through the inversion analysis with from observed phase velocity data with the layered structure models. Distributions of layer boundary depths were estimated from the results and gravity survey data. 2-D 3rd-order B-spline function was adopted for modeling boundary depth distribution. Strong ground motions due to the 1943 Tottori earthquake (M7.2) was simulated by the 3-D finite difference method. The 3-D subsurface structure model was well verified by comparing the distribution of peak ground velocity with the damage distribution under the 1943 Tottori earthquake.

Keywords: strong ground motion, 3-D finite difference method, Tottori plain, 3-D subsurface structure

## Development of numerical program for rigid body rotation

IMAEDA, Yusuke<sup>1\*</sup>, MORIKAWA, Hitoshi<sup>1</sup>

<sup>1</sup>Tokyo Tech

We developed a numerical calculation program for rigid body rotation. Tombstone is widely distributed object and becomes a good recorder of earthquake, since it slips, rotates, falls down, and jumps, affected by the earthquake motion. Therefore, it is important to investigate the motion of tombstone or rigid body rotation, numerically.

When we develop the numerical program for rigid body rotation, we have to be careful about the orthogonality and the unity of the unit vector along the principal axis of inertia. Conservation of energy and the angular momentum is also important. A simple numerical program does not ensure these properties.

Our program represents the time evolution as the summation of rotations. Since the exact rotation does not break the orthogonality and the unity of the unit vector, the summation of these rotations also does not break these properties. Rotation can be represented by quaternion. To ensure the conservation properties, we consider the time evolution of the unit angular momentum vector on the rigid body frame. On this frame, the unit angular momentum vector moves along the closed curve, which is determined by the given energy.

The comparison between our program and the other simple program will be presented.

Keywords: simulation, rigid body

## Determination of subsurface structure in urban area of Tottori city using microtremors.

ASAHI, shugo<sup>1\*</sup>, Kazunori Makimoto<sup>1</sup>, NOGUCHI, Tatsuya<sup>1</sup>, KAGAWA, Takao<sup>1</sup>

<sup>1</sup>Graduate School of Engineering, Tottori University

Serious damages occurred by the strong ground motions during the 1943 Tottori earthquake in Tottori city. Microtremor observations were carried out in the area, a subsurface determined structure by Noguchi et al. (2003),(2006). In this study, the predominant period at 226 sites were obtained from 3-componet observation records. As a result, H/V spectra were classified from spectral shape and vale. A predominant period distribution map was obtained. In north of Tottori station, predominant period was long; 0.8~1.1 second and sediment layer was thick; 35~48m. In south of Tottori station, predominant period was short; 0.1~0.3 second and sediment layer was thin; 11~15m.

Keywords: Microtremor observation, H/V, Tottori city, subsurface structure

## Development of a low power consumption strong motion observation system

YOSHIMOTO, Kazuo<sup>1\*</sup>, SHIGETA, Takanori<sup>2</sup>, NAKAHARA, Hisashi<sup>3</sup>, SATO, Hiroshi<sup>4</sup>

<sup>1</sup>Nanobioscience, Yokohama City Univ., Yokohama, Japan, <sup>2</sup>International College of Arts and Sciences, Yokohama City Univ., Yokohama, Japan, <sup>3</sup>Geophysics, Science, Tohoku Univ, Sendai, Japan, <sup>4</sup>ERI, Univ. of Tokyo, Tokyo, Japan

Recent studies on seismic wave analysis have found that the seismic basement structure hidden beneath a thick sedimentary layer can be investigated by the seismic interferometry of strong motion records. In order to obtain strong motion records at as many points as possible, we developed a low power consumption strong motion observation system.

The strong motion observation system consists of electronic parts for consumer market applications, such as a digital triaxial MEMS acceleration sensor, ultralow-power 16-bit microcontroller, and SD card device. The MEMS acceleration sensor allows high accurate measurement of accelerations with  $\pm 1.5G$  full scale and 14-bit resolution. The noise level is 4 gal in p-p amplitude, approximately. The 16-bit microcontroller monitors the acceleration signals with 40 Hz sampling rate, and makes a trigger for event recording when the monitor signals exceed a certain level. The recording signal is 64 s in length, including 15 s pre-trigger part. The recording capacity of SD card device is 2G byte. The new strong motion observation system consumes 2mA or less, and operates over several months by using 4 alkaline D-size batteries.

A test observation to evaluate the availability of the new strong motion observation system shows that this system is useful for recording strong motion with an intensity of 3 and over on the JMA seismic intensity scale.

Keywords: strong motion observation system, MEMS acceleration sensor, low power consumption

## Source model of the 2011 East Shizuoka prefecture, Japan, earthquake by using the empirical Green's function method

SOMEI, Kazuhiro<sup>1\*</sup>, MIYAKOSHI, Ken<sup>1</sup>, KAMAE, Katuhiro<sup>2</sup>

<sup>1</sup>G.R.I., <sup>2</sup>KURRI

On March 15, 2011, an inland crustal earthquake ( $M_{JMA}6.4$ , Strike slip type) occurred in the east Shizuoka prefecture, Japan. A strong ground motion of about  $1000\text{cm/s}^2$ ,  $70\text{cm/s}$  was recorded at the nearest strong motion station, SZO011, about 20 km away from the hypocenter. Maeda and Sasatani (2009) showed that a similar large ground motion of  $1100\text{cm/s}^2$ ,  $75\text{cm/s}$  at HKD020 during the 2004 South Rumoi district, Japan, inland crustal earthquake ( $M_{JMA}6.1$ , Dip slip type) is mainly attributable to the source effect, short distance from the strong motion generation area (SMGA) and the forward directivity effect. To investigate the factors of this large ground motion at SZO011 from a source's point of view, we estimate the source model by strong motion simulations. The source model is constructed based on the forward simulations using the empirical Green's function method (Irikura, 1986) in the frequency range between 0.3Hz and 10Hz. One rectangle SMGA is estimated to include the rupture start point that is a hypocenter of the mainshock determined by Japan Metro Agency. The rupture of this SMGA mainly propagates from deep side to shallow side for dip direction, and also propagates bi-laterally for strike direction. The obtained source model explains the observed acceleration, velocity, and displacement waveforms of this event in the broadband frequency range fairly well. The parameters of this SMGA are consistent with the previous studies for inland crustal earthquakes (e.g., Miyake *et al.*, 2003).

On the other from site's point of view, we compare observed seismograms at SZO011 with those of SZOH37 that is close to the SZO011 station and located on the rock site. For a variety of earthquakes, the spectral levels at SZO011 tend to larger than those of SZOH37. Strong ground motion was affected not only directivity effects but also large site response at SZO011. The site response of the mainshock based on the S-wave horizontal-to-vertical spectral ratio method (e.g., Noguchi and Sasatani, 2011) shows the non-linearity for the frequency range from 3 Hz to 5 Hz. However, the site response shows linearity for other small earthquakes.

### Acknowledgements

We would like to sincerely thank NIED (K-NET, KiK-net, F-net) for providing the strong motion data. The hypocenter information was providing by JMA and moment tensor by F-net of NIED. This study was supported by Nuclear Safety Commission of Japan (NSC).

Keywords: 2011 East Shizuoka prefecture, Japan, earthquake, strong ground motion, empirical Green's function method, source model

## Two-dimensional Velocity Structure Inversion Using the Voxel FEM

GUO, Yujia<sup>1\*</sup>, KOKETSU Kazuki<sup>1</sup>

<sup>1</sup>Earthquake Research Institute, The University of Tokyo

In order to clarify the characteristics and mechanism of strong ground motions, it is essential to evaluate the effects of not only the source process of an earthquake but also the velocity structure where seismic waves propagate. In particular, the heterogeneity and anelastic attenuation of a velocity structure are thought to cause seismic waveforms to vary significantly. Therefore, we must reconstruct a reliable velocity structure model whose heterogeneity and anelastic attenuation are sufficiently reflected. In this study, we propose a new method to determine a two-dimensional velocity structure with heterogeneity and anelasticity, by performing a waveform inversion for P-SV wave propagation.

In the forward procedure, we use the voxel finite-element method (FEM) (Koketsu et al., 2004). A voxel mesh can be generated easily and fast, thus it is possible to compute seismograms by the use of almost the same amount of memory and time as a finite difference method (FDM). To each rectangular mesh, we apply the Galerkin scheme and use shape functions for the first-order element. We discretize in the time domain with central and backward-difference schemes for the term of acceleration and velocity, respectively. In this two-dimensional problem, a seismic source should be a line source. Consequently, we transform approximately the line source into a point source, using the approach of Hikima (2007).

For the purpose of fulfilling broadband attenuation, we introduce Rayleigh damping (Ikegami 2009), which is the linear combination of stiffness-proportional damping and mass-proportional damping. This enables the required constant-Q spectra to be satisfied for P and SV-wave.

Because of nonlinearity of the inversion problem presented here, which is constrained least-squares optimization problem, it is solved iteratively so that its regional optimum solutions satisfy Karush-Kuhn-Tucker (KKT) condition. Our optimization approach is based on that of Askan (2006) and Askan et al.(2007). For calculating partial differential seismograms, we perform partial differentiation directly for optimality system and forward procedure simultaneously. We use the reduced optimization space approach which is feasible for the large-scale problem we consider. We choose the step length by solving the first-order minimization problem, called line search technique. We then determine the search direction with the Newton-CG method, where the Newton direction is found by making the Gauss-Newton approximation and employing the conjugate gradient (CG) method. In order to overcome multiple local minima, we use the multi-grid algorithm, in which we repeat the inversion procedure by initially solving the solution on a coarse material grid and then utilizing the solution as an initial guess for the next finer grid.

In this presentation, we show the detail of methodology of our work and the result of numerical experiment with it.

Keywords: Velocity structure, Attenuation, Finite-element method (FEM), Inversion

## Possibility of the Microtremor Observation and Structural Health-Monitoring by using IT Kyoshin seismometer

ITO, Takamori<sup>1\*</sup>, SHIDA, Ryutaro<sup>2</sup>, TAKANO, Kiyoshi<sup>3</sup>

<sup>1</sup>ERI, The University of Tokyo, <sup>2</sup>GSFS, The University of Tokyo, <sup>3</sup>ERI, The University of Tokyo

In order to reduce the seismic disaster, it seems to be the usefulness to investigate the seismic vibration of our familiar buildings such as housing, companies, schools, etc. in small earthquake, examine the weak point and improve the earthquake resistance of these building effectively. For this purpose, we devised IT strong motion seismometer as a new type self install strong motion seismometer.

In order to promote widely usage, the development of the IT strong motion sensor was performed with emphasis on lowering a price rather than the sensor sensitivity.

Therefore, it was thought that we could not use it for the microtremor observation.

However, in Shida et. al (2011), it was shown that the same peak frequency was detectable by using the IT strong motion sensor as the high-sensitive sensor when it was set an upper-layers story.

We could recognize that we are able to use IT strong motion sensor for microtremore observation of the building, and for structural health monitoring also.

Thereby, we have checked the change of the building vibration characteristic due to the 2011 off the Pacific coast of Tohoku Earthquake for the buildings which were installed IT strong motion sensors.

It was confirmed that a natural frequency of buildings is changed at the 2011 off the Pacific coast of Tohoku Earthquake in many buildings. We will report some changes by the repair of the damaged buildings also.

Keywords: IT Kyoshin (Strong Motion) Seismometer, Structural Health Monitoring



## Investigation of NFRD effect on strong ground motion during the 2004 Rumoi earthquake (Mj 6.1) using the Hybrid method

MIYAKOSHI, Ken<sup>1\*</sup>, NISHIMURA, Toshimitsu<sup>1</sup>, SASATANI, Tsutomu<sup>2</sup>, KAMAE, Katuhiro<sup>3</sup>

<sup>1</sup>GRI, <sup>2</sup>Former Hokkaido Univ., <sup>3</sup>KURRI

Rupture directivity effects cause spatial variations in strong ground motions amplitude near the fault. An inland crustal earthquake (Mj 6.1) occurred on December 14, 2004 in the northern part of Hokkaido, Japan (2004 Rumoi earthquake). Source mechanism is reverse fault type with low dip angle (Dip=25degree). A strong ground motions over 1000 cm/s<sup>2</sup> and 70 cm/s were recorded at the nearest strong-motion station (HKD020) about 10 km from the hypocenter. Using EGF (Empirical Green's Function) method, Maeda and Sasatani (2009) concluded that the large strong ground motions at HKD020 are mainly affected by forward directivity effects and shallow asperity. Miyakoshi et al.(2010) also validated these effects using theoretical method.

In this study we investigate NFRD (Near Fault Rupture Directivity) effect on strong ground motion during the 2004 Rumoi earthquake using the Hybrid simulation, which is combined of 3D-FD and SGF (Stochastic Green's Function) method. We calculated seismograms near the fault area (20km x 20km) and made PGV distribution map. Strong ground motion over 70cm/s, which are affected by NFRD (Near Fault Rupture Directivity) effect, are appeared around the surface projection line of the upper edge of the rupture area. We tried to extract area of the NFRD effect on near-source strong ground motions using the criteria of Ohno et al. (1998). They showed that the predominant area of the NFRD effect for the reverse fault type is defined an area having size  $\pm 0.25L$  and centered on the projection of the upper edge of rupture, where L is length of the surface projection line. Additionally we tried to choose large PGV zone in the predominant area of the NFRD effect using PGV attenuation curve (Si and Midorikawa, 1999). We selected the large PGV zone that has PGV greater than average PGV +1 sigma. As a result, we successfully chose large PGV zone affected by the NFRD effect near the fault area.

### Acknowledgements

We would like to sincerely thank NIED (K-NET, KiK-net, F-net) for providing the strong motion data. The hypocenter information was providing by JMA and moment tensor by F-net of NIED. This study was supported by Nuclear Safety Commission of Japan (NSC).

Keywords: 2004 Rumoi earthquake, strong ground motion, hybrid simulation, NFRD effect

## Estimation of shallow velocity structure by seismic interferometry of microtremor

YASUDA, Hironobu<sup>1\*</sup>, SEKIGUCHI, Haruko<sup>1</sup>

<sup>1</sup>DPRI, Kyoto Univ.

Recently, seismic interferometry (for example, Wapenaar and Fokkema, 2006), which is the method to get Green's function between two sites by cross correlating recordings of the wave filed at the two sites, is used for many analysis. It is also applied to investigate sedimentary layer structures. For example, Yamanaka and Uchiyama (2008) conducted the microtremor measurement in the Matsumoto basin, and obtained group velocity of surface wave and estimated the S wave velocity structure. In our study, we conducted microtremor array measurements with several tens of meter spacing and examine the applicability of seismic interferometry to investigate shallow subsurface sedimentary structure in detail.

The target are of our microtremor measurements is Uji campus, Kyoto University. In the past, various kinds of subsurface structure exploration have been done in and around the Uji Campus. P wave seismic reflection exploration and borehole survey to investigate the Oubaku fault running near the Uji campus (Koizumi et al., 2002) have shown velocity profile under the Uji campus up to about 500m deep. From the surface down, P wave velocity gradually increases from 1500 to 2500m/s, and sharply rises over 3000m/s at around 400m deep. Layer structure is clear beneath the campus.

We conducted microtremor measurement on 8th and 9th March, 2011. We put 10 SMAR strong-motion seismometers in a line array, and recorded 15-minute-long microtremor data for 10 times, so we got totally 150-minute-long record, on each day. We set sampling rates 200Hz, and the seismometers were placed about 30m apart, and recorded 3 components data. Then, we applied seismic interferometry to these records. Frequency components higher than 0.2Hz can be used for the analysis judging from the Fourier spectra of the data. We prepared 30 segments of 30-seconds-long window from each 15-minutes-long record. We calculated cross-correlation functions of the records between one endmost station and other 9 stations and stacked them for 300 times. By arranging the stacked cross-correlation functions according to the distance between stations, we see clear propagation of wave packet along the measurement line. We will also discuss the character of the wave packet and its propagation velocity.

## Antakya Basin Strong Ground Motion Network

OZEL, Oguz<sup>1\*</sup>, Eser Cakti<sup>2</sup>, Murat Bikce<sup>3</sup>, Cemal Genes<sup>3</sup>, Selcuk Kacin<sup>3</sup>

<sup>1</sup>Istanbul University, <sup>2</sup>Bogazici University, <sup>3</sup>Mustafa Kemal University

Antakya Basin Strong Ground Motion Network was established in 2009 with the objectives of monitoring the earthquake response of the Antakya Basin, improving our understanding of basin response, assisting to determine the effects of local and regional earthquakes on the urban environment of Antakya and contributing to its earthquake risk assessment of Antakya, that is a town in southeastern Turkey marked with high earthquake hazard and historical and cultural significance. The system is the first of its kind in Turkey with the primary purpose of monitoring basin response.

The network consists of six instruments installed in small buildings. The stations form a straight line along the short axis of Antakya basin passing through the city center. They are equipped with acceleration sensors, GPS and communication units and operate in continuous recording mode. The soil properties beneath the strong motion stations (S-Wave velocity structure and dominant soil frequency) are determined by array measurements.

A number of regional earthquakes have been recorded by the system since its installation. Following preliminary observations can be deduced from their analysis and from the results of array measurements (1) to the west of river Asi, average bedrock depth is 480m. The depth of engineering bedrock is estimated as 250m; (2) ground motion amplification along the short-axis of the basin can clearly be observed from the recordings; (3) to the west of the Asi River, 3 to 10 times amplifications in ground motion levels are observed. They tend to increase as one moves towards the middle of the basin.

Our immediate plan is to increase the number of stations to twelve with the intention of covering areas of the basin along its long axis and to carry out further geophysical and geotechnical studies to better characterize the velocity structure within the basin.

Keywords: Strong Motion, Antakya Basin, Earthquake Risk Assessment